RSC Advances

PAPER

View Article Online
View Journal | View Issue

Cite this: *RSC Adv.*, 2025, **15**, 6050

Chemoselective synthesis of tunable poly-functionalized binary pyrazolyl and annulated pyrazolo/pyrido anchored on quinolinone: insecticidal and antioxidant studies†

Nedaa N. Elnaggar,[a] Wafaa S. Hamama, *[a] M. Abd El Salam[b] and Eslam A. Ghaith [ac]

The present work is directed to synthesize new tolerance binary pyrazolylquinolinone such as pyrazolylquinolinone, 1-phenylpyrazolyl)quinolinone and 1,2,4-triazolyl)pyrazolyl)quinolinone and fused pyrazolo-/pyridoquinolinone hybrids as pyrazolo[4,3-*c*]quinolinone, benzo[*h*][1,6]naphthyridinedione, tetrahydrobenzo[*h*][1,6]naphthyridine-3-carbonitrile and 2,7-triazaindeno[4,5,6-*de*]anthracenol as prospective ingredients with the aim of assessment for their antioxidant and insecticidal potentiality. Additionally, *in vitro* and *in vivo* insecticidal bio-responses, cotton leafworm, *Spodoptera littoralis* (*S. littoralis*) and the cotton aphid were screened for the synthesized compounds. Interestingly, the most potent compounds were **11** and **5** with (LC_{50} 119.79 and 164.63 mg L^{-1}) against *S. littoralis*. Furthermore, the influence of the tested compounds on biochemical parameters, including AChE, ATPase, total protein levels, detoxifying enzymes CaE, and GST were also inspected. Furthermore, the targeted compounds showed promising antioxidant activity comparable with ascorbic acid as the presence of both of functionalized quinolinone and pyrazole moieties increasing the scavenger radical inhibition. Finally, DFT calculations were implemented to investigate the electronic and structural properties of the synthesized scaffolds.

Received 17th December 2024
Accepted 11th February 2025

DOI: 10.1039/d4ra08834d

rsc.li/rsc-advances

1. Introduction

Quinoline skeletons, as multifaceted platforms found in numerous alkaloids, are widely present in plants, marine organisms, and microorganisms. In addition, quinolinone derivatives have evoked high importance due to their utilization as antimicrobials, antivirals, herbicides and fungicides in agrochemistry[1–6] as shown in Fig. 1. Consequently, quinolinone derivatives are considered as key privileged scaffolds in discovery and development of pesticides.[7,8] Among functionalized quinolinones, 4-hydroxyquinolinone and its derivatives are of significant interest in both chemical and medicinal domains. Whereby, the broad-spectrum biological activities greatly increase the flexibility of quinoline structure modification and derivatization providing great potential for the discovery of new novel quinolinone entities as new insecticides. In addition, recent reports have underscored that enaminones derived from hydroxyquinolinone moiety display potential larvicidal and molluscicidal activities against schistosomiasis at transmission stages.[9,10]

On the other hand, pyrazoles are well-known pharmacophores that have played an important role in the discovery of new pesticides, such as cyenopyrafen, furametpyr, tebufenpyrad, cyantraniliprole and fenpyroximate as marketed pesticides have a great interest for a new crop protection (Fig. 1).[11–15] So that, our target to design and synthesis of entities pyrazole binary or fused to show a significant assemblage motif for pharmacological candidates that are widely utilized in agricultural crop protection as exhibiting considerable insecticide and acaricide activities as in recent literature.[8,13–15]

Moreover, the insecticidal toxicity of the cotton leafworm, *Spodoptera littoralis* (*S. littoralis*) and the cotton *aphid* has been very important for the discover new insecticides because insects are serious in initiating inclusive crop damages owing to their herbivorous environment and/or being disease routes.[16–18] These arthropods are responsible for reducing universal food assembly by 20% in addition to decreasing domestic nutrition security at the post-harvest level.[19,20] Whereas, the cotton leaf worm, *S. littoralis* (*Boisduval*, order; lepidoptera, family; Noctuidae) is one of the utmost hurtful and destructive *Noctuid* pests invading about 90 plant species concerning to 40 plant

[a]*Chemistry Department, Faculty of Science, Mansoura University, Mansoura, 35516, Egypt. E-mail: wshamama@mans.edu.eg; wshamama53@gmail.com*
[b]*Plant Protection Research Institute, ARC, Dokki, Giza 12619, Egypt*
[c]*Chemistry Department, Faculty of Science, New Mansoura University, New Mansoura City, Egypt*

† Electronic supplementary information (ESI) available. See DOI: https://doi.org/10.1039/d4ra08834d

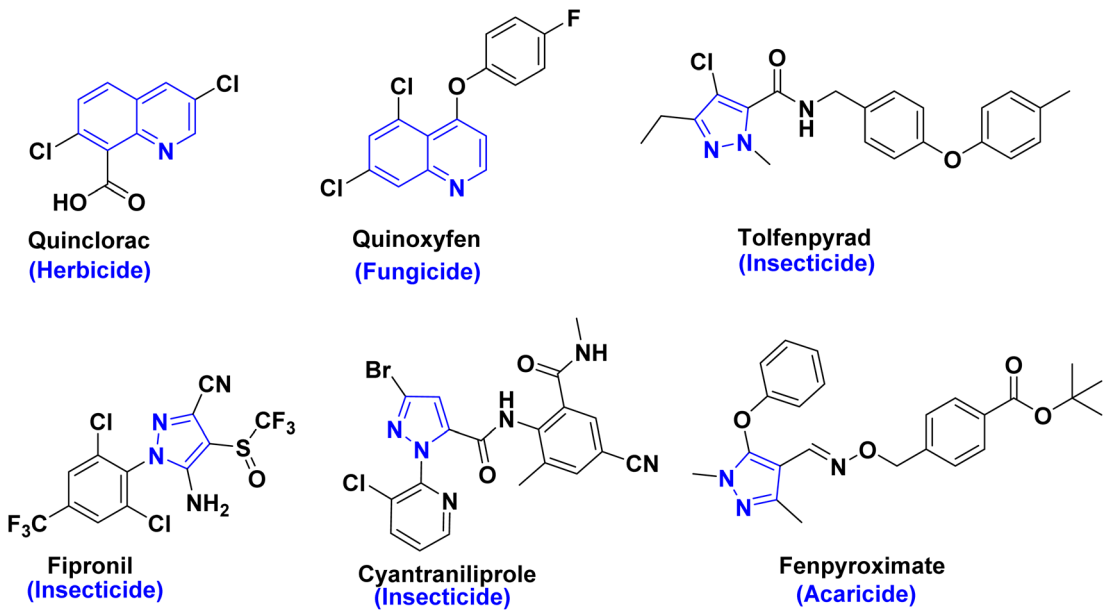

Fig. 1 Commercial pesticides and insecticides that contain pyrazole or quinolinone compounds.

families containing cotton, as one of the most main economic crops in the world.[21,22] Therefore, many agriculture organizations recommend using potent chemical pesticides to reduce their population due to their potential impact on ecological balance and public health, which leads to serious fear of future impacts.[23]

Also, the cotton aphids, are capable of transmitting plant viruses *i.e.* plant pathogens.[24,25] *Aphis gossypii Glover* (Hemiptera: Aphididae), is a significant sucking polyphagous pest with numerous hosts causing plenty of agricultural injuries by hasty reproduction,[26–28] through excretion honeydew causing various fungal diseases and viral transmission in plants.[29] Nevertheless, the overuse of insecticides has led to the development of resistance of *A. gossypii* to the most marketed insecticides.[30] Consequently, the synthesis of innovative, long-lasting biologically active pesticides with different biological mechanisms is a talented tactic to discover novel pesticides for combating and decreasing insecticidal-resistant infections.[31,32]

Whereby, the hybridization concept offers a fascinating strategy for developing novel, safe, and effective pesticides.[33,34] As the hybrid ligands (bitopic ligands) are class of scaffolds consisting of two functional pharmacophores conjoining by linker into a single molecule.[35,36] Whereby, adjoining of two potent molecules provides numerous approaches for creation innovative potential interaction efficacy with less pesticidal resistance susceptibility.[36] Consequently, the application of insecticidal activities for the innovation of new molecular hybridization between quinolinone and pyrazole pharmacophores has been shown for the first time. By combining pyrazole and quinoline moieties, we aim to create new hybrid molecules that leverage the synergistic features of both pharmacophores, targeting multiple biological pathways. As pyrazoles have two different electronegativity nitrogen atoms that could act as either hydrogen donors or acceptors, enabling access to improving the polarity of the targeted molecules.[37]

Whereas, quinoline contains a benzene ring that acts as a lipophilic fragment for neuroreceptor binding, boosting drug-likeness and solubility profiles.[37,38] This strategy is expected to enhance insecticidal activity and improve solubility profiles, ultimately leading to more potent and effective control of polyphagous pests like the cotton leafworm.[39] Herein, this manuscript focuses on the integration of the quinoline framework with pyrazole derivatives, which offers numerous advantages in the discovery and development of potent and effective new pesticides.

2. Results and discussion

2.1. Chemistry: synthesis and structural characterization

As part of our research into the synthesis of novel heterogeneous hybrids[40–42] we designed and prepared a new series of quinolinone-based pyrazoles by straightforward one-pot reaction methodology. This direct strategy offers various merits involving mild conditions and eco-friendly approach which follows the green synthesis rules. Today, one of the important missions of organic synthesis is converting easily available building blocks into high value-added products and if possible, with an environmentally friendly approach. Among these starting materials, enaminone **1** was utilized as effective synthon for constructing valuable heterocyclic compounds. In our strategy, acetyl quinolinone is rapidly treated by molar equivalent of *N*,*N*-dimethylformamide dimethyl acetal (DMF-DMA) under thermal condensation to give pure (*E*)-3-(3-(dimethylamino)acryloyl)-4-hydroxy-1-phenylquinolin-2(1*H*)-one(enaminone) (**1**) with excellent yield.[9]

Whereby, the reactivity of the enaminone scaffolds can be attributed to the incorporation of the electrophilicity of enones

and nucleophilicity of enamines;[43] therefore the chemical reactivity of enaminone **1** has been explored towards nucleophilic hydrazine derivatives. Initially, cyclocondensation of enaminone **1** with hydrazine hydrate ($NH_2NH_2 \cdot 2H_2O$) in boiling ethanol in presence of acetic acid yielded the corresponding pyrazolylquinolinone derivative **2** in 87% yield (Scheme 1). In accordance with the presence of its three tautomeric possibilities namely **2a–c**, the suggested tautomeric forms were investigated *via* density function studies (DFT) in liquid state. These studies supported the assumption that tautomer **2a** predominates over another tautomers due to two rational factors (a) tautomer **2a** is found to be more chemically stable (lower total energy, −27441.92 eV) than other tautomers (−27441.83 and −27 441.83 eV, Fig. 2), based on the electron density calculations (b) hydrogen bond (H–B) in tautomer **2b** (1.876 Å) is stronger than H·B in other tautomers **2a** and **2c** (2.238 and 2.028 Å, respectively), supported our assumption as less stable tautomers form stronger hydrogen bonds according to perturbation theories[44,45] (Fig. 2).

The constitution of compound **2** was confirmed by its ^{1}H NMR spectrum, which displayed the absence of two singlet signals of two *N*-methyl groups at δ = 2.94 and 3.27 ppm in parent enaminone **1** [A data availability statement (DAS)], and two exchangeable singlet signals attributed to OH and NH protons appeared at δ 13.45 and 14.12 ppm. Whereas, its IR spectrum showed one characteristic band for lactamic carbon at 1629 cm^{-1} and atrophy of carbonyl group related to enaminone. Similarly, the acidic mediated reaction of enaminone **1** with phenyl hydrazine yielded the corresponding pyrazolylquinolinone **3** in 82% yield (Scheme 1). The skeleton of binary pyrazolylquinolinone derivative **3** was secured based upon different spectral analyses, as ^{1}H NMR spectrum revealed exchangeable singlet signal at δ = 11.04 ppm assignable for OH function, and multiplet signals at δ = 6.49–8.01 ppm corresponding to aromatic protons of three phenyl and pyrazole rings. Additionally, ^{1}H and ^{13}C NMR confirmed the formation of the suggested product through the disappearance of two aliphatic methyl groups in our starting material. Whereas, ^{13}C NMR spectrum of **3** supports the existence of two signals in deshielding region at 161.0 and 159.7 ppm attributed to carbon in position 4 and lactamic carbon in the quinolinone nucleus. To provide an additional evidence of our scoped strategy, treatment of enaminone **1** with 4-amino-5-hydrazineyl-4*H*-1,2,4-triazole-3-thiol (**4**) as a multifunctionality precursor for various hydrazino hybrid was performed. The sol product was obtained as golden yellow flakes in 87% yield and identified as 5-mercapto-4*H*-1,2,4-triazol-1*H*-pyrazolo-1-phenyl-quinolinone **5** (Scheme 1).

EI-MS reinforced the constitution of compound **5** due to the appearance of its molecular ion peak at *m*/*z* 417.03, which was compatible with its molecular weight. Also, ^{1}H NMR spectrum of designated **5** confirmed the presence of three exchangeable singlet signals at δ = 5.86, 13.07, and 14.15 ppm related to NH_2, OH and SH, respectively. Whereas, ^{13}C NMR spectrum confirmed the absence of signals attributed to two methyl groups N–CH_3 and C=O of enaminone. Additionally, the most

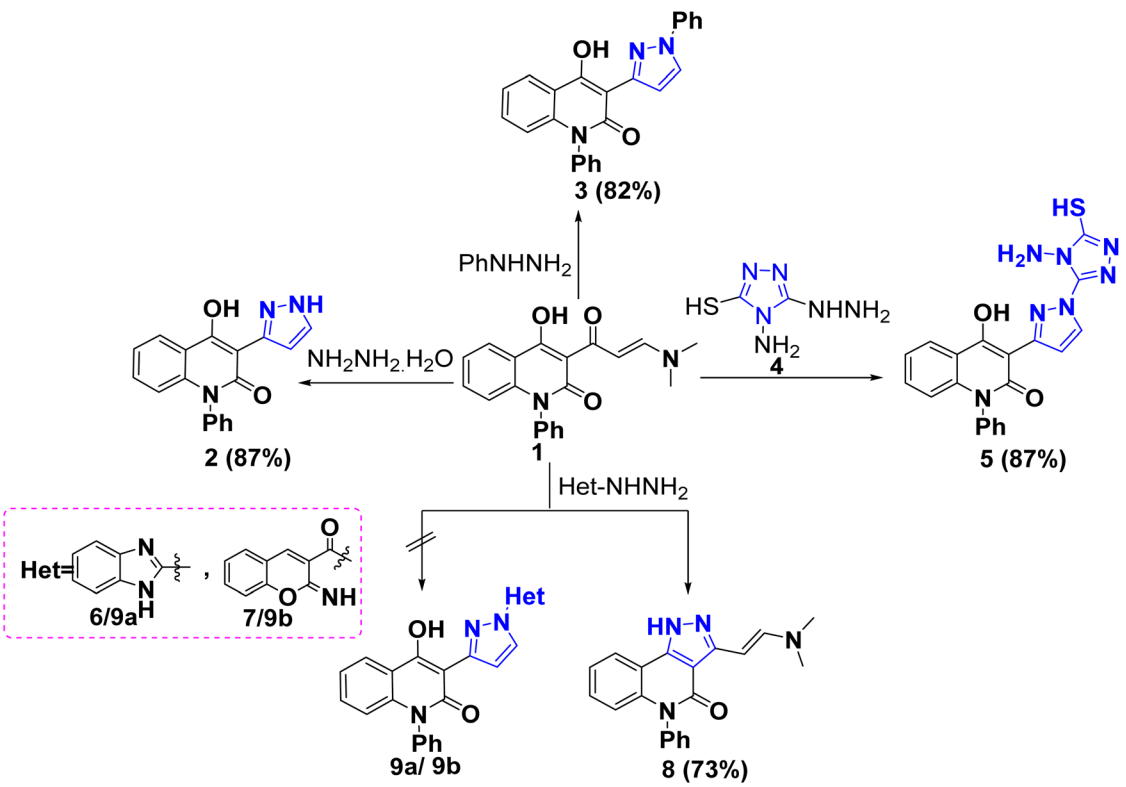

Scheme 1 Treatment of enaminone **1** with different hydrazines.

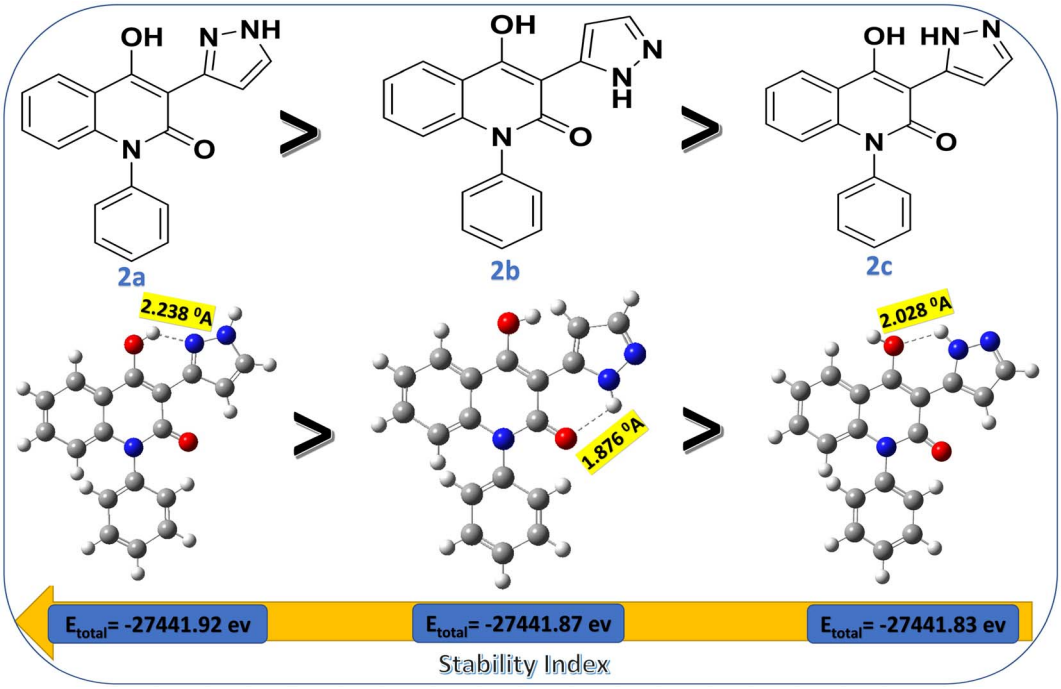

Fig. 2 Total energies and H·B lengths of the optimized geometrical tautomers **2a–c**.

characteristic intense carbon signals resonate at δ 167.3, 160.9, 160.5 and 151.4 and 144.0 ppm assignable to C–SH, C–OH, C=O and two C=N, respectively. Whereby, the other thirteen signals at δ 139.9, 137.7, 132.5, 132.0, 130.0, 129.3, 128.7, 123.8, 122.2, 115.4, 114.8, 108.7 and 99.4 are attributed to sp^2 hybridized carbons.

A plausible reaction mechanism involving hydrazines react with enaminone **1** through the selective 1,2-Michael-addition pathway not *via* 1,4-Michael addition and generates the intermediate A. Then volatile dimethylamine could be eliminated, giving the desired selective pyrazoles **2**, **3** and **5**. The selectivity of the reaction between enaminone **1** and the hydrazines (Scheme 2) towards 1,2-Michael addition is more favorable than 1,4-Michael addition pathway according to the DFT calculations. This is due to the carbonyl group polarizing effect on the acidic medium (AcOH). Where, AcOH lowers the free energy barrier for the 1,2-addition pathway, which results in a lower activation energy compared to other routes because of the formation of unsaturated imine. But, the 1,4-addition reaction involves the direct nucleophilic attack of the hydrazine group on the activated position of enaminone, which occurs at a slower kinetic step and limiting reaction ability to yield competitive kinetics for imine formation.[46–48]

While, the treatment of enaminone **1** with heterocyclic hydrazine with 2-hydrazinyl-1*H*-benzo[*d*]imidazole (**6**) afforded chemoselective (*E*)-3-(2-(dimethylamino)-5-phenyl-4*H*-pyrazolo

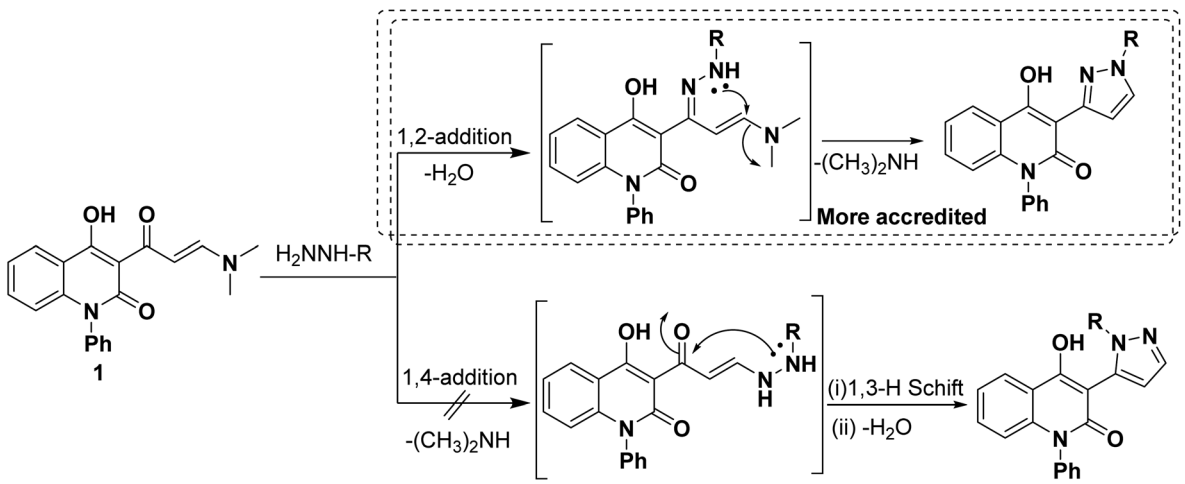

Scheme 2 The mechanistic pathway of reaction of **1** with R-NHNH$_2$.

[4,3-*c*]quinolin-4-one (**8**) instead of anticipated skeleton **9**. The spectroscopic analyses (IR, ^{1}H, ^{13}C NMR and EI-MS) have been elucidating the constitution of the annulated pyrazoloquinolinone **8**. As its ^{1}H NMR spectrum showed two singlet signals at $\delta = 2.93$ and 3.26, alongside the presence of the characteristic two adjacent methine groups (2CH) at $\delta =$ 7.51 and 8.09 ppm with the same $J_{coupling} = 7$ Hz, as well as the absence of the hydroxyl group at C_4 of quinolinone. Whereby, its ^{13}C NMR spectrum displayed two upfield signals at $\delta = 45.5$ and 37.6 ppm due to sp^3 hybridized carbon atoms attributed to magnetic nonequivalent two methyl carbons. Whereby, the IR spectrum revealed only one characteristic carbonyl band related to lactamic carbonyl (C_2) at 1634 cm^{-1}. In addition, EI-MS spectrum revealed its molecular ion peak (M^+) at $m/z = 330.52$ which was in accordance with its molecular formula $C_{20}H_{18}N_4O$.

The rational explanation for the formation of annulated product **8** instead of expected compound **9b** was discussed according to the retrosynthesis mechanism (Scheme 3). The proposed pathway included condensation of hydrazido group to carbonyl which enolized from OH group at C_4 yielded non-isolable intermediate **8A** followed by its retro dissociation to salicylaldehyde and intermediate **8B**. Next, intramolecular nucleophilic attack of NH functionality to the carbonyl group followed by ring transformation, simultaneous decarboxylation process of intermediate **8C**. For elucidate our hypothesis, we examined the reaction proceeding and comparing TLC with the intended standard sample of salicylaldehyde, revealing the elimination of salicylaldehyde during the reaction (Scheme 3). We think that this phenomenon can be attributed to undergo of an effective amino group of hydrazido function to imino tautomerism, rendering them poor nucleophiles due to the delocalization of lone pair on nitrogenous atom.[49]

The scope of utilization of enaminone was extended through different reaction profile, by performing a reaction of enaminone **1** with triethylenetetramine (TETA) as highly active linear polyamines (as zigzag structure) due to less steric effects as its linear nature supports its ability to twist and rotate.[50] This reaction was carried out in CH_2Cl_2 and led to the formation of 1-methyl-6-phenyl-benzo[*h*][1,6]naphthyridine-4,5(1*H*,6*H*)-dione (**10**) instead of transamination products. Whereas, ^{1}H NMR spectrum supported the skeleton **10**, as showed upfield singlet signal attributed to the methyl group (N–CH_3) at $\delta = 2.70$ ppm, and two doublet signals corresponding to methine hydrogens in pyridinone ring at $\delta = 6.50$ and 8.18 ppm with $J_{coupling} = 8$ Hz. Whereas, its ^{13}C NMR showed a total 14 signals identified as one upfield signal at δ 31.3 characteristic for methyl group and eleven signals at δ 142.9, 137.8, 135.6, 130.5, 129.7, 129.3, 125.7, 122.9, 116.2, 114.7, 106.3 for olefinic and aromatic carbons, besides two new signals at δ 174.6 and 206.8 corresponding to highly downfield two carbonyl groups which are compatible with the suggested structure. Whereas, IR spectrum confirmed the structure of constitution **10** revealing the absence of a hydroxy group. The proposed mechanism for the formation of compound **10** can be rationalized through TETA acts as a precursor of methyl amine *via* dissociation of TETA.[51]

Then the methyl amine attacks the electrophilic α-carbon of the enaminone system leading to transamination process, followed by cyclization and elimination of the water molecule yielding the fused benzonaphthyridindione **10**.

The reaction of enaminone **1** with *C*-nucleophile such as malononitrile was examined in refluxing AcOH led to the formation of (*E*)-4-(2-(dimethylamino)vinyl)-2,5-dioxo-6-phenyl-1,2,5,6-tetrahydrobenzo-[*h*][1,6]naphthyridine-3-carbonitrile (**11**). The formation of structure **11** can be rationalized through condensation of the carbonyl group with active methylene according to 1,2-addition mechanism, then the nucleophilic attack of OH functionality to the cyano group was achieved, followed by Dimorth rearrangement, instead of an alternative path involving displacement of active methylene to the dimethylamino group as an anticipated route. The skeleton **11** was established based on its spectral data, as its IR spectrum showed a strong absorption band at 2225 cm^{-1} related to the nitrile group. Moreover, ^{1}H NMR confirmed the proposed

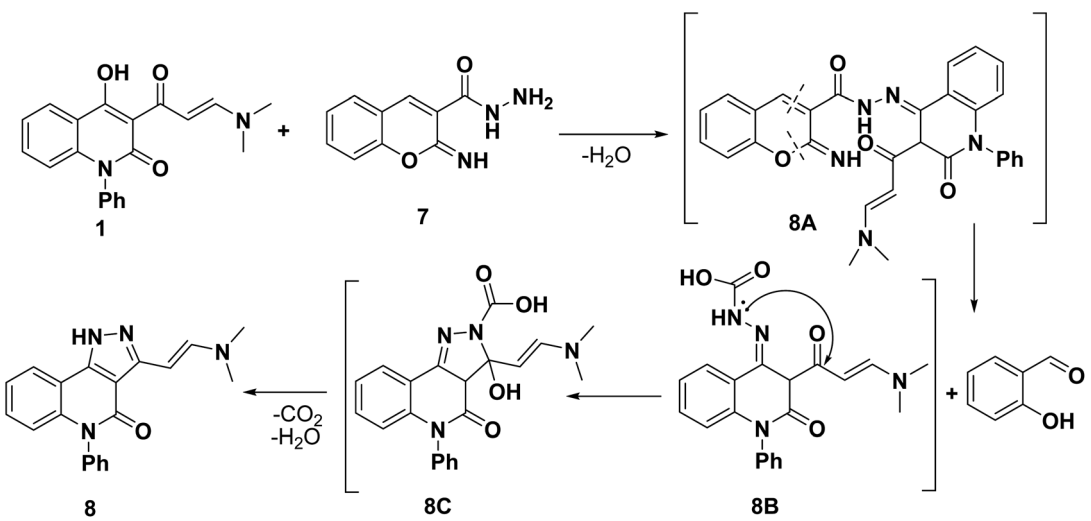

Scheme 3 Reasonable retrosynthesis mechanism for the formation of **8**.

structure due to the presence of two singlet signals attributed to two methyl groups at 2.93 and 3.27 ppm, whereby their carbons resonated at 37.7 and 45.5 ppm in ^{13}C NMR analysis. Whereby, EI-MS spectrum revealed a peak at *m*/*z* 382.68 corresponding to its molecular ion. The scope of reaction 5-methyl-2,4-dihydro-3*H*-pyrazol-3-one (**12**) as heterocyclic *C*-nucleophile was investigated *via* the reaction of enaminone **1** with pyrazolone **12** in AcOH under the refluxing condition yielding 3-methyl-7-phenyl-6,12-dioxa-1,2,7-triazaindeno[4,5,6-*de*]anthracen-11*b*(7*H*)-ol (**13**) (Scheme 4). The proposed pathway of the formation of skeleton **13** involved a condensation reaction of the methylene group of pyrazole moiety and enaminone carbonyl group yielded 1,5 dicarbonyl intermediate **13A**, followed by *in situ* tautomerization and cyclization reactions including enolic OH group attacks the endo-ketonic carbonyl group of quinolinone, whereas, another OH group at position 2 attacks β-position of enaminone which extensively activated and influenced by the conjugated system led to elimination of dimethyl amine molecule produced fused polycyclic system **13** as final product (Scheme 4). FT-IR and ^{1}H NMR spectra of compound **13** displayed the disappearance of methylene protons of the pyrazole moiety, showing one upfield singlet signal at $\delta = 2.30$ ppm corresponding to the methyl group of the pyrazole ring. In addition, a broad signal at 3.37 ppm is attributed to the alcoholic OH group contaminated with H_2O of DMSO. Besides, its mass spectrometry displayed a peak at *m*/*z* 369.43 due to its molecular ion that agrees with its molecular formula $C_{22}H_{15}N_3O_3$.

2.2. Biological activity

2.2.1. Toxicological efficacy assessment for 2nd, 4th larvae of *S. littoralis* and cotton aphid. The freshly synthesized binary and fused pyrazoloquinolones were estimated for *in vitro* insecticidal action against the 2nd and 4th instar larvae of *S. littoralis*. Whereby, LC_{50} values of the examined compounds exhibited a significant toxicity after a 72 h of feeding on castor leaves treated with tested compounds *via* leaf-dip bioassay as accessible in Table 1. Whereas, $LC_{50,s}$ values for 2nd instar larvae were 119.79, 164.63, 228.69, 339.92, 421.04, 601.34, 855.41 and 1164.73 ppm for compounds **11**, **5**, **13**, **3**, **1**, **10**, **8** and **2**,

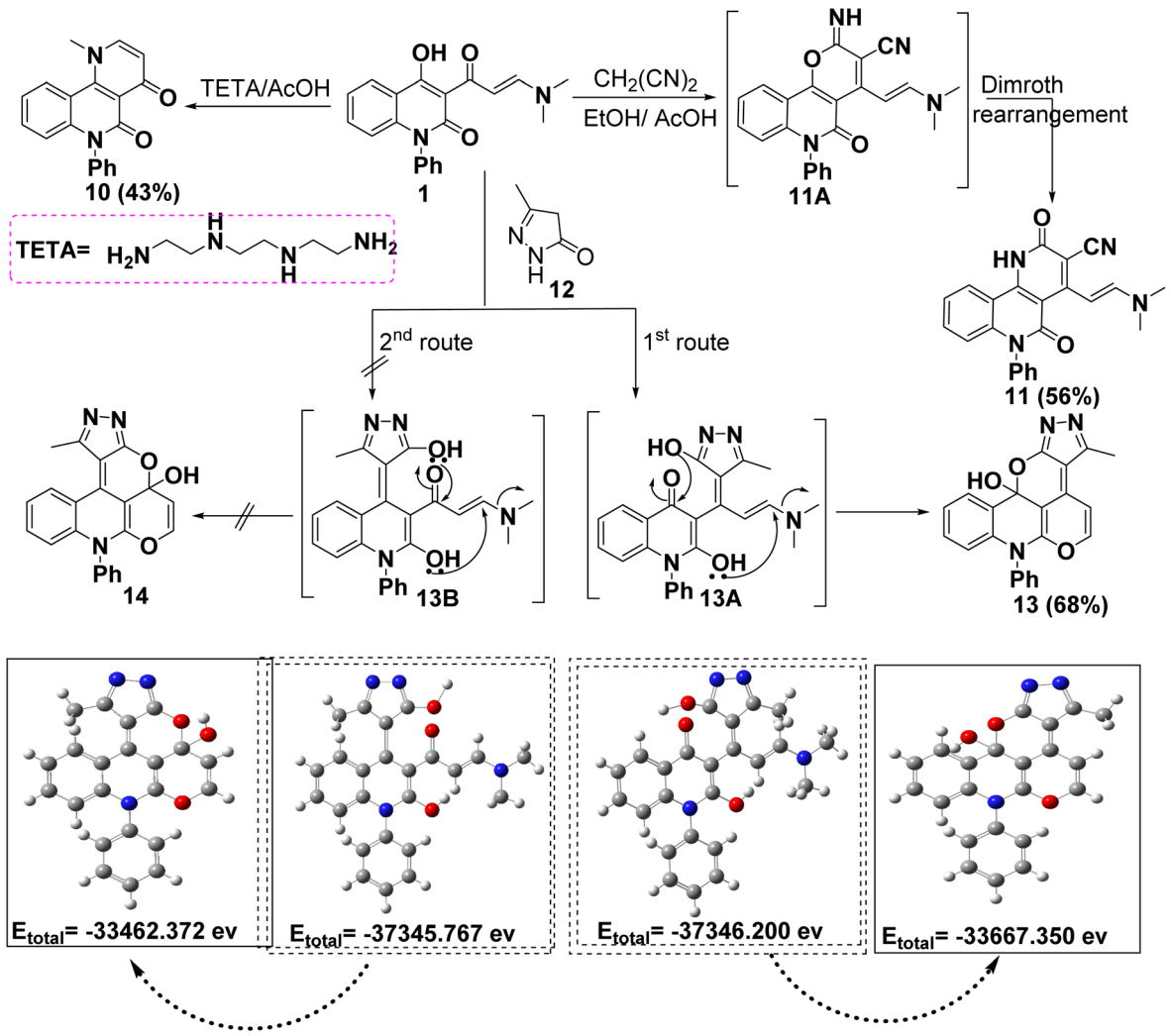

Scheme 4 Synthesis of compounds **10**, **11** and **13**.

Table 1 *In vitro* insecticidal efficacy of the investigated scaffolds towards the 2nd and 4th instar larvae of *S. littoralis* by the leaf-dip technique after 3 days of the treatment

Tested compounds	2nd instar larvae				4th instar larvae			
	LC_{50} (ppm) and confidence limits at 95%	LC_{25} (ppm) and confidence limits at 95%	Slope	Toxicity index % at LC_{50} value	LC_{50} (ppm) and confidence limits at 95%	LC_{25} (ppm) and confidence limits at 95%	Slope	Toxicity index % at LC_{50} value
11	**119.785** 86.876, 162.493	**44.761** 26.035, 64.182	1.578 ± 0.224	**100**	**292.520** 210.971, 406.345	**89.504** 54.596, 129.225	1.312 ± 0.152	**100**
5	**164.628** 123.202, 216.745	**62.782** 40.605, 86.763	1.611 ± 0.180	**72.76**	**425.842** 291.569, 626.602	**111.475** 57.211, 173.083	1.159 ± 0.168	**68.69**
13	**228.690** 170.307, 309.454	**84.622** 54.720, 116.971	1.562 ± 0.190	**52.38**	**643.055** 449.026, 971.652	**176.178** 100.403, 261.457	1.200 ± 0.172	**45.49**
3	**339.923** 242.827, 472.656	**113.163** 65.152, 165.390	1.412 ± 0.191	**35.24**	**918.989** 606.203, 1570.290	**217.850** 98.022, 348.084	1.079 ± 0.202	**31.83**
1	**421.041** 288.276, 590.435	**136.257** 67.384 209.940	1.377 ± 0.214	**28.45**	**1350.084** 898.118 2460.767	**354.476** 193.266, 533.546	1.161 ± 0.214	**21.67**
10	**601.339** 423.071, 862.103	**191.181** 101.836, 285.562	1.355 ± 0.212	**19.92**	**2024.150** 1344.135 3498, 017	**495.627** 237.133, 775.916	1.104 ± 0.204	**14.45**
8	**855.411** 613.888, 1259.479	**283.047** 166.778, 406.032	1.404 ± 0.217	**14.00**	**2928.858** 1959.785, 5334.542	**808.260** 463.412, 1197.422	1.206 ± 0.216	**9.99**
2	**1164.727** 803.508, 1881.462	**362.516** 173.757, 547.581	1.331 ± 0.268	**10.28**	**4028.479** 2501.453 10, 350.049	**971.798** 418.765, 1541.172	1.092 ± 0.267	**7.26**

respectively and the toxicity index being 100, 72.76, 52.38, 35.24, 28.45, 19.92, 14.00 and 10.28%, respectively. In the same context, $LC_{50,s}$ values for 4th instar larvae after a 72 h exposure were 292.52, 425.84, 643.06, 918.99, 1350.08, 2024.15, 2928.86 and 4028.48 ppm for **11**, **5**, **13**, **3**, **1**, **10**, **8** and **2**, respectively and the toxicity index being 100, 68.69, 45.49, 31.83, 21.67, 14.45, 9.99 and 7.26%, respectively. While, this study indicates binary and fused pyrazole derivatives demonstrate more effectiveness against *S. littoralis* compared to some reported spiro nitrogenous heterocyclic scaffolds.[52] This postulate can be attributed to various possible factors (a) regarding to the configuration, spiro constitutions possess a stiff three-dimensional configuration with restricted capacity for hitting active site of the receptor target protein. (b) Conversely, fused pyrazolo scaffolds show more planar with less restricted conformation, facilitating interaction with the biological target with flexible orientation of the functional groups.[53]

Whereas, the laboratory bioassay was conducted for estimating the efficacy of eight newly synthesized quinolone scaffolds as toxic agents towards the neonate nymphs of the phytophagous, *A. gossypii* Glover (Table 2). After 24 h of treatment, all tested scaffolds demonstrated acceptable toxic potency when compared to trademarked insecticide, acetamiprid 20% SP (LC_{50} 4.88 ppm, 100% toxicity index). Whereby, targeted compounds **11**, **5**, **3**, **13**, **1**, **10**, **8** and **2** exhibits excellent results with $LC_{50,s}$ values 7.67, 9.70, 10.77, 12.17, 13.94, 18.76, 30.42 and 41.72 ppm, respectively, and the toxicity index being 63.64, 50.31, 45.30, 40.09, 35.02, 26.02, 16.04 and 11.70%, respectively.

2.2.2. Biochemical parameters. Adenosine triphosphatases (ATPases) are vital enzymes that regulate various physiological processes in insects, including: molting and development through ion and solute transport during molting, ensuring proper cuticle formation and development and regulating insect behavior such as feeding and mating.[54–56] Besides, they are essential for glucose transportation and they are situated in the midgut, malpighian tubules and nerve fibers of the pest.[56] In addition, ATPases reduce the effectiveness of chemicals such as bacillus thuringiensis (Bt) toxins boosting their insecticide resistance through genetic mutations. Additionally, they control thermoregulation during physiological processes.[54,55]

On the other hands, glutathione *S*-transferases (GSTs) are essential enzymes in insects, playing key roles in: (a) detoxifying insecticides, plant toxins, and other xenobiotics, reducing their toxicity; (b) maintaining antioxidant defenses against reactive oxygen species (ROS); (c) contributing to insecticide resistance by metabolizing the insecticide; (d) regulating cell signaling and development: influencing insect development, growth, and reproduction.[57–59] Whereby, carboxylesterases (CAEs) contribute to insect resistance to various insecticides, including: organophosphates, pyrethroids and carbamates. CAEs are enzymes that play crucial roles in insect physiology including: (a) insecticide metabolism by hydrolyzing ester bonds in insecticides, reducing their potency; (b) xenobiotic detoxification of foreign compounds, such as plant toxins; (c) regulating lipid metabolism, influencing energy and reproduction; (d) degrading pheromones, controlling behavior and communication.[60–63]

Table 2 Susceptibility of the *A. gossypii* to the synthesized pyrazoloquinolones as insecticidal agents compared by acetamiprid, 20% SP after 24 h of treatment

Tested compounds	LC_{50} (ppm) and confidence limits at 95%	LC_{90} (ppm) and confidence limits at 95%	Slope	Toxicity index % at LC_{50} value
Acetamiprid 20% SP	**4.881**	**19.807**	2.107 ± 0.487	**100**
	2.282, 6.854	14.762, 35.967		
11	**7.670**	**40.010**	1.786 ± 0.486	**63.64**
	2.095, 12.048	28.517, 89.503		
5	**9.702**	**60.206**	1.617 ± 0.398	**50.31**
	3.504, 14.656	41.538, 143.834		
3	**10.774**	**76.372**	1.507 ± 0.387	**45.30**
	3.830, 16.174	49.520, 237.319		
13	**12.174**	**96.129**	1.428 ± 0.380	**40.09**
	4.444, 18.015	58.285, 398.891		
1	13.938	119.869	1.371 ± 0.374	35.02
	5.426, 20.241	67.838, 673.102		
10	**18.758**	**180.075**	1.305 ± 0.370	**26.02**
	8.984, 26.339	89.157, 1836.854		
8	**30.424**	**232.245**	1.452 ± 0.393	**16.04**
	21.450, 44.283	108.808, 2498.205		
2	**41.715**	**309.274**	1.473 ± 0.344	**11.70**
	31.569, 60.016	151.112, 1985.754		

Consequently, understanding GSTs and CaE in insects can inform the development of novel insecticides and resistance management strategies. Whereas, the total proteins in insects can provide valuable insights into their biology, behavior, and ecology, ultimately informing the development of innovative pest management strategies. These proteins perform several critical functions: (a) regulate the growth, and reproduction; (b) catalyze metabolic reactions to produce energy; (c) defend against pathogens and parasites and enable adaptation to environmental changes. Overall, these biological aspects involve intricate mechanisms and signaling pathways that govern key systems essential for insect survival and adaptation. Therefore, inhibiting these biological aspects in *S. littoralis* leads to the elimination or reduction of their populations.

Whiley, the LC_{50} values obtained from leaf-dip application of the most potent toxic tested pyrazoloquinolones were utilized to evaluate the effects on some biochemical responses. Survived larvae from each treatment were selected, then weighed, and used for the assessment of total protein and activity of acetylcholinesterase (AChE), adenosine triphosphate (ATPase), total protein, detoxifying enzymes (CaE), and glutathione *S*-transferase (GST). Whereas, effect of the LC_{50} values acquired from the leaf-dip method of the newly established synthetic compounds on AChE demonstrated that pyrazoloquinolones **11** was the utmost inhibitory action followed in the descending order by **5**, **13** and **3**, respectively compared to the standardized cholinesterase activity (Table 3). Controlled cholinesterase activity was significantly decreased from 0.771 OD (mg protein)$^{-1}$ min^{-1} to 0.331, 0.413, 0.507 and 0.605 OD (mg protein)$^{-1}$ min^{-1} in larvae treated with **11**, **5**, **13** and **3**, respectively with significant differences between them and the untreated larvae. However, AChE activity levels were considerably increased due to the starting compound **1** (0.953 OD per mg protein per min), higher than the control by 23.61%. Additionally, the *in vivo* inhibitory controls of LC_{50} values of treatments against adenosine triphosphatase (ATPase) of 4th instar larvae of *S. littoralis* were reported in Table 3. Considerably, each insecticide reduced normalized ATPase activity compared to the untreated larvae. Compound **11** induced the ultimate reduction in the activity of ATPase (0.448 OD (mg protein)$^{-1}$ min^{-1}), significantly lower than in the control (0.853 OD (mg protein)$^{-1}$ min^{-1}), followed by **5**, **13** and **3** at 0.518, 0.598 and 0.692 OD (mg protein)$^{-1}$ min^{-1}, respectively. However, compound **1** cause a significant increase in ATPase levels by 4.57% than the control to 0.892 OD (mg protein)$^{-1}$ min^{-1}. Whereas, data in Table 3 indicated that compound **11** recorded the ultimate reduction in the activity of the detoxifying enzyme glutathione *S*-transferase (GST) of 4th instars larvae of *S. littoralis* treated by leaf-dip technique at 0.214 mg per protein per min, significantly lower than in the control (0.520 OD (mg protein)$^{-1}$ min^{-1}) by −58.85%, followed by **5**, **13** and **3**, at 0.312, 0.410 and 0.468 mg per protein per min, respectively lower than control, respectively, while the considerably increase in GST activity was induced by **1** (0.723 OD (mg protein)$^{-1}$ min^{-1}) by 39.04% higher than the normalized GST activity in the control referring that this enzyme is a detoxifying enzyme of xenobiotics at low concentrations.

In the same context, a noteworthy *in vivo* decrease of detoxifying enzyme carboxylesterase CaE was established in the larvae with LC_{50} values of different inspected insecticides compared to the control (0.315 mg per protein per min) as documented in Table 3. Though, the larvae treated with **11**, **5**, **13** and **3** have lower activity of CaE (0.098, 0.151, 0.188 and 0.250 OD (mg protein)$^{-1}$ min^{-1}, respectively). Whereby, compounds, **5** and **13** have no significant difference in CaE activity between each other. Conversely, compound **1** showed a proper increase in CaE activity at 0.452 OD (mg protein)$^{-1}$ min^{-1} by 43.49% comparing with normalized CaE in the untreated larvae. From

Table 3 *In vivo* biochemical effects in hemolymph of 4th instar larvae of *S. littoralis* after 5 days of treatment for the utmost potent toxic scaffolds **11**, **5**, **13**, **3** and **1**

Treatments	LC_{50} (mg L^{-1})	Enzyme activity (OD (mg protein)$^{-1}$ min^{-1}) ± SE									
		AChE	% Cont.	ATPase	% Cont.	GST	% Cont.	CaE	% Cont.	Total protein	% Cont.
11	**292.520**	0.331 ± 0.012	**−57.07**	0.448 ± 0.007	**−47.48**	0.214 ± 0.006	**−58.85**	0.098 ± 0.006	**−68.89**	0.331 ± 0.010	−68.63
5	**425.842**	0.413 ± 0.010	**−46.43**	0.518 ± 0.009	**−39.27**	0.312 ± 0.006	**−40.00**	0.151 ± 0.011	**−52.06**	0.433 ± 0.010	**−58.96**
13	**643.055**	0.507 ± 0.009	**−34.24**	0.598 ± 0.006	**−29.89**	0.410 ± 0.008	**−21.15**	0.188 ± 0.004	**−40.32**	0.508 ± 0.009	**−51.85**
3	**918.989**	0.605 ± 0.008	**−21.53**	0.692 ± 0.004	**−18.87**	0.468 ± 0.007	**−10.00**	0.250 ± 0.023	**−20.63**	0.605 ± 0.008	**−42.65**
1	**1350.084**	0.953 ± 0.023	**23.61**	0.892 ± 0.012	**4.57**	0.723 ± 0.006	**39.04**	0.452 ± 0.013	**43.49**	1.135 ± 0.009	**7.58**
Untreated larvae	—	0.771 ± 0.028		0.853 ± 0.002		0.520 ± 0.008		0.315 ± 0.009		1.055 ± 0.014	
LSD 0.05		**0.052**		**0.034**		**0.021**		**0.039**		**0.032**	

Fig. 3 *In vivo* biochemical effects in hemolymph of 4th instar larvae of *S. littoralis*.

the outcomes in Table 3, it can be detected that all the examined compounds caused a remarkable reduction in the activity of total proteins in 4th instars larvae of *S. littoralis* by 0.331, 0.433, 0508 and 0.605 per mg per protein per min for **11**, **5**, **13** and **3**, respectively compared with the untreated larvae (1.055 OD (mg protein)$^{-1}$ min^{-1}) except compound **1**, showed an increase by 7.58% at 1.135 OD (mg protein)$^{-1}$ min^{-1} than the control in total protein content (Fig. 3).

For biochemical impacts on *A. gossypii* enzymes, the results revealed that all the tested pyrazoloquinolones compounds displayed a significant susceptibility to Acetylecoline esterase AChE activity (Table 4). The enzyme activity reached its minimum value in *A. gossypii* nymphs treated with LC_{50} of Acetamiprid 20% SP treatment (0.106 OD (mg protein)$^{-1}$ min^{-1}) comparing with the untreated nymphs (0.253 OD (mg protein)$^{-1}$ min^{-1}) followed in the descendent order by pyrazoloquinolones **11**, **5**, **3**, **13** and **1**, respectively at 0.134, 0.153, 0.183, 0.215 and 0.253 OD (mg protein)$^{-1}$ min^{-1} respectively compared to the standardized cholinesterase activity. Likewise, we observed that there was a considerably *in vivo* inhibitory action in Adenosine triphosphatase ATPase activity when nymphs of *A. gossypii* treated by LC_{50} values of the tested insecticides comparing with control group (Table 4, Fig. 4). Controlled ATPase activity was significantly reduced from 0.282 OD (mg protein)$^{-1}$ min^{-1} to 0.170, 0.203, 0.228, 0.244, 0.258 and 0.278 OD (mg protein)$^{-1}$ min^{-1} in nymphs treated with LC_{50} of Acetamiprid 20% SP, **11**, **5**, **3**, **13** and **1**, respectively with significant differences between them and the standardized group. In addition, data in Table 4 indicated that *A. gossypii* nymphs treated with LC_{50} of Acetamiprid 20% SP recorded a significant decrease in the bioresponse of the detoxifying enzyme GST at 0.023 OD (mg protein)$^{-1}$ min^{-1} considerably lower than in the untreated nymphs (0.128 OD (mg protein)$^{-1}$ min^{-1}) by −82.03%, followed by quinolinones **11**, **5**, **3**, **13** and **1**, at 0.043, 0.063, 0.083, 0.103 and 0.121 OD (mg protein)$^{-1}$ min^{-1}, respectively (Fig. 4). As well, a noteworthy *in vivo* reduction of detoxifying enzyme carboxylesterase CaE was recognized in the nymphs of *A. gossypii* treated with LC_{50} values of different inspected insecticides compared to the control (0.106 OD (mg protein)$^{-1}$ min^{-1}) as acknowledged in Table 4. However, the nymphs treated with Acetamiprid 20% SP, **11**, **5**, **3**, **13** and **1** had

Table 4 *In vivo* biochemical effects on nymphs of *A. gossypii* after 24 h of treatment at LC_{50} values of the most potent toxic quinolinones **11**, **5**, **3**, **13** and **1** compared with the Acetamiprid 20% SP

		Enzyme activity (OD (mg protein)$^{-1}$ min^{-1}) ± SE									
Treat	LC_{50} (mg L^{-1})	AChE	% Cont.	ATPase	% Cont.	GST	% Cont.	CaE	% Cont.	Total protein	% Cont.
Acetamiprid 20% SP	**4.881**	0.106 ± 0.005	**−58.10**	0.170 ± 0.001	**−39.72**	0.023 ± 0.002	**−82.03**	0.013 ± 0.002	**−87.74**	0.199 ± 0.003	**−43.63**
11	**7.67**	0.134 ± 0.002	**−47.04**	0.203 ± 0.008	**−28.01**	0.043 ± 0.002	**−66.41**	0.02 ± 0.003	**−81.13**	0.271 ± 0.002	**−23.23**
5	**9.702**	0.153 ± 0.001	**−39.53**	0.228 ± 0.002	**−19.15**	0.063 ± 0.002	**−50.78**	0.042 ± 0.001	**−60.38**	0.282 ± 0.001	**−20.11**
3	**10.774**	0.183 ± 0.002	**−27.67**	0.244 ± 0.002	**−13.48**	0.083 ± 0.002	**−35.16**	0.061 ± 0.002	**−42.45**	0.308 ± 0.002	**−12.75**
13	**12.174**	0.215 ± 0.002	**−15.02**	0.258 ± 0.002	**−8.51**	0.103 ± 0.003	**−19.53**	0.081 ± 0.001	**−23.58**	0.321 ± 0.002	**−9.07**
1	**13.938**	0.235 ± 0.003	**−7.11**	0.278 ± 0.002	**−1.42**	0.121 ± 0.001	**−5.47**	0.094 ± 0.003	**−11.32**	0.340 ± 0.003	**−3.68**
Untreated nymphs	—	0.253 ± 0.002		0.282[a] ± 0.001		0.128 ± 0.002		0.106 ± 0.002		0.353 ± 0.003	
LSD 0.05		**0.009**		**0.008**		**0.006**		**0.006**		**0.007**	

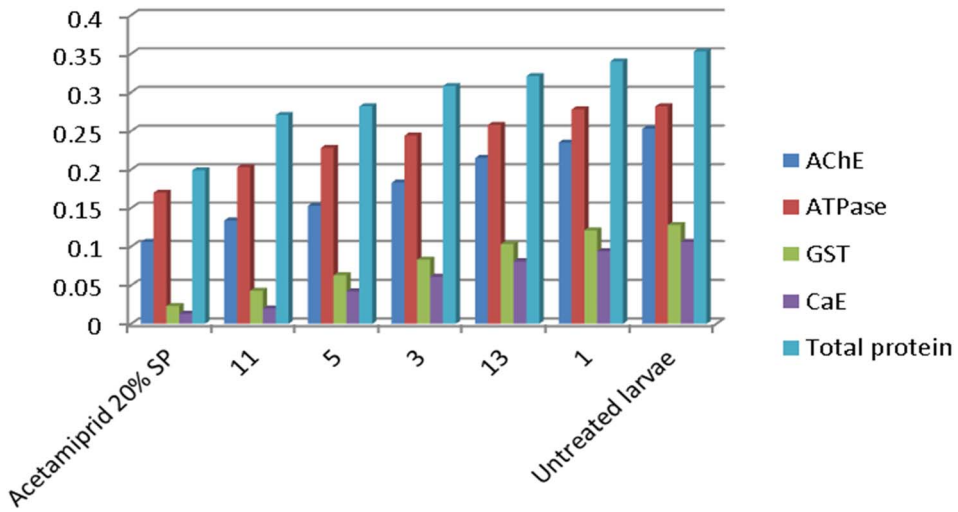

Fig. 4 *In vivo* biochemical effects for tested compounds in the nymphs of *A. gossypii*.

a proper lower activity levels of CaE at 0.013, 0.020, 0.0.042, 0.061, 0.081 and 0.094 OD (mg protein)$^{-1}$ min^{-1}), respectively.

All the examined compounds caused a proper decrease in the activity of total proteins in nymphs of *A. gossypii* treated with LC_{50} values of different examined insecticides by 0.199, 0.271, 0.282, 0.308, 0.321 and 0.340 OD (mg protein)$^{-1}$ min^{-1} for acetamiprid 20% SP, **11**, **5**, **3**, **13** and **1**, respectively compared with the standardized total proteins levels (0.353 OD (mg protein)$^{-1}$ min^{-1}) as tabulated in Table 4 (Fig. 4).

The biological parameters of *S. littoralis* were studied; as the freshly molted 4th instar larvae were allowed to survive on caster leaves treated with LC_{25} of the furthest persuasive toxic quinolinones, **11**, **5**, **13**, **3** and **1** for 48 h and untreated leaves until pupation. The main biological measurements were authenticated in Tables 5 and 6. For larval and pupal duration, all the examined quinolinones prompted a proper elongation in the larval duration comparing with the untreated larvae (10.60 days), recorded as 22.90 days for compound **11**, 19.49 days for compound **5**, 17.37 days for compound **13**, 14.52 days for compound **3** and 10.40 days with a considerably difference among them and the control group except compound **1** has no significance to the untreated larvae (Table 5 and Fig. 5). Contrariwise, the pupal duration was considerably reduced (Table 5). Quinolinones, **11**, **5**, **13**, **3** and **1** established 8.18, 9.26, 10.36, 11.41 and 12.72 days, respectively compared with the standardized larvae (13.10 days) as illustrated in Fig. 6. Furthermore, the most effective inspected quinolinone scaffolds produced a noteworthy reduction of the pupal weight with significant changes between them, where **11** was the supreme active, 258.42 mg, compared to the untreated larvae (300.67 mg), followed in the descending order by the recently synthesized synthetic compounds **5**, **13**, **3** and **1**, respectively (269.23, 277.10, 285.42 and 297.39 mg, respectively) as accessible in Table 5 and Fig. 5.

As regards the latent effects on the 4th instar larvae of *S. littoral* with LC_{25} of most potent toxic new quinolinones, the data authenticated in Table 5 exposed that compound **11** was the furthermost dynamic, recording 33.51%, 15.91%, and

Table 5 Effects of the highly toxic evaluated synthetic pyrazoloquinolinones **11**, **5**, **13**, **3** and **1** using leaf-dip technique at their LC_{25} values on some biological aspects of the laboratory strain of the 4th Instar Larvae of *S. littoralis*

Treatments	LC_{25} (mg L^{-1})	Larval duration (days)	Pupal duration (days)	Pupal weight (mg)	Normal pupae (%)	Deformed pupae (%)	Adult emergence (%)
11	**89.504**	$22.90^{a} \pm 0.265$	$8.18^{e} \pm 0.101$	$258.42^{e} \pm 1.496$	$33.51^{e} \pm 0.369$	$15.91^{a} \pm 0.332$	$62.96^{f} \pm 0.289$
5	**111.475**	$19.49^{b} \pm 0.198$	$9.26^{d} \pm 0.195$	$269.23^{d} \pm 0.576$	$44.80^{d} \pm 0.282$	$14.47^{b} \pm 0.265$	$65.99^{e} \pm 0.294$
13	**176.178**	$17.37^{c} \pm 0.261$	$10.36^{c} \pm 0.121$	$277.10^{c} \pm 0.878$	$54.48^{c} \pm 0.504$	$11.75^{c} \pm 0.450$	$72.44^{d} \pm 1.502$
3	**217.850**	$14.52^{d} \pm 0.219$	$11.41^{b} \pm 0.206$	$285.42^{b} \pm 0.366$	$69.46^{b} \pm 0.399$	$9.68^{d} \pm 0.216$	$78.49^{c} \pm 0.860$
1	**354.476**	$10.40^{e} \pm 0.529$	$12.72^{a} \pm 0.126$	$297.39^{a} \pm 1.398$	$93.92^{a} \pm 0.261$	$5.00^{e} \pm 0.468$	$89.90^{b} \pm 0.808$
Untreated larvae	—	$10.60^{e} \pm 0.493$	$13.10^{a} \pm 0.203$	$300.67^{a} \pm 1.17$	$94.46^{a} \pm 0.084$	$3.42^{f} \pm 0.240$	$93.57^{a} \pm 0.751$
LSD 0.05		**1.088**	**0.507**	**3.279**	**1.055**	**1.058**	**2.634**

Table 6 Effects of the highly toxic evaluated synthetic quinolinones at their LC_{25} values on fecundity, fertility and adult longevity for surviving 4th Instar karvae of *S. littoralis*

					Adult longevity (days)	
Treatments	LC_{25} (mg L^{-1})	No. of eggs/female	Fecundity (%)	Egg hatchability (%)	Male	Female
11	**89.504**	$731.67^{f} \pm 9.26$	$25.41^{f} \pm 0.222$	$43.67^{f} \pm 0.295$	$4.95^{d} \pm 0.072$	$6.93^{e} \pm 0.046$
5	**111.475**	$827.33^{e} \pm 6.89$	$28.73^{e} \pm 0.189$	$54.17^{e} \pm 0.107$	$6.96^{c} \pm 0.036$	$10.17^{d} \pm 0.220$
13	**176.178**	$1014.33^{d} \pm 11.57$	$35.23^{d} \pm 0.379$	$61.81^{d} \pm 0.351$	$9.07^{b} \pm 0.185$	$10.58^{d} \pm 0.300$
3	**217.850**	$1326.33^{c} \pm 6.96$	$46.06^{c} \pm 0.256$	$74.27^{c} \pm 0.517$	$9.79^{b} \pm 0.137$	$11.61^{c} \pm 0.201$
1	**354.476**	$1907.67^{b} \pm 13.92$	$66.25^{b} \pm 0.670$	$87.60^{b} \pm 0.776$	$12.61^{a} \pm 0.282$	$12.85^{b} \pm 0.163$
Untreated larvae	—	$2879.67^{a} \pm 11.62$	100^{a}	$98.37^{a} \pm 0.320$	$13.32^{a} \pm 0.437$	$15.58^{a} \pm 0.363$
LSD 0.05		**31.931**	**1.074**	**1.374**	**0.722**	**0.733**

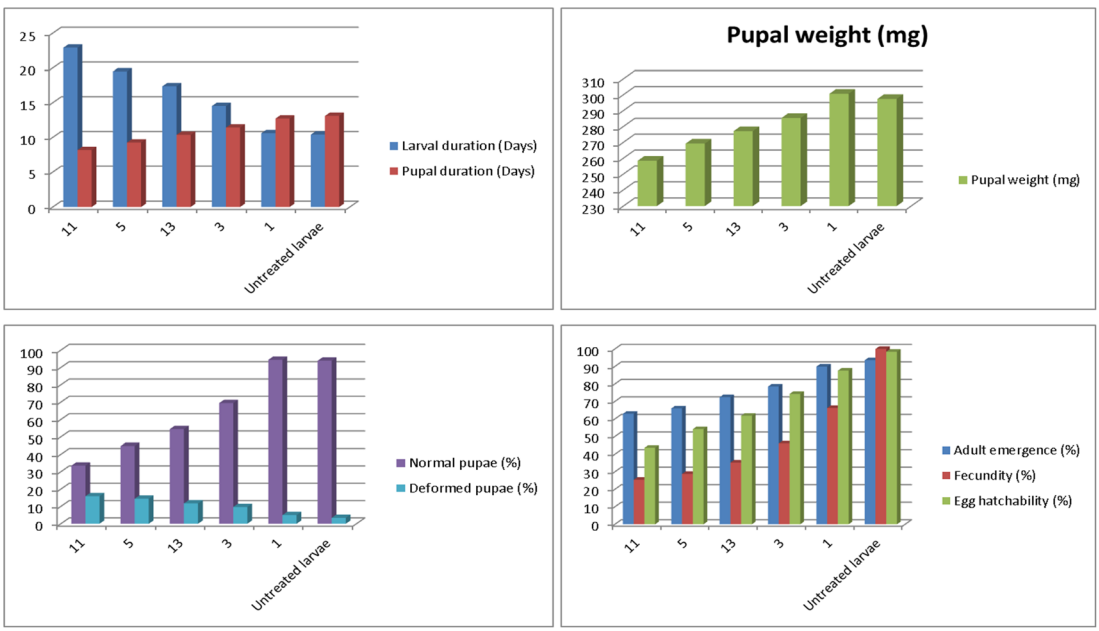

Fig. 5 Effects of the pyrazoloquinolones **11**, **5**, **13**, **3** and **1** at their LC_{25} values on biological parameters of *S. littoralis*.

62.96%, respectively, of normal pupae, deformed pupae, and adult emergence, compared to the untreated larvae (93.92%, 3.42%, and 93.57%, respectively), followed by **5** (44.80%, 14.47% and 65.99%), **13** (54.48%, 11.75% and 72.44%), **3** (69.46%, 9.68% and 78.49%) and **1** (94.46%, 5.00% and 89.90%) as illustrated in Fig. 5. With regard to the data symbolized in Table 6, number of eggs per female, percentage of fecundity, and percentage of egg hatchability, we concluded that, the newly established pyrazoloquinolinones **11**, **5**, **13**, **3** and **1** had stimulated remarkably significant reduction of the mean numbers of eggs produced by adult females (fecundity) and as well egg hatchability (fertility) was harshly reduced in the

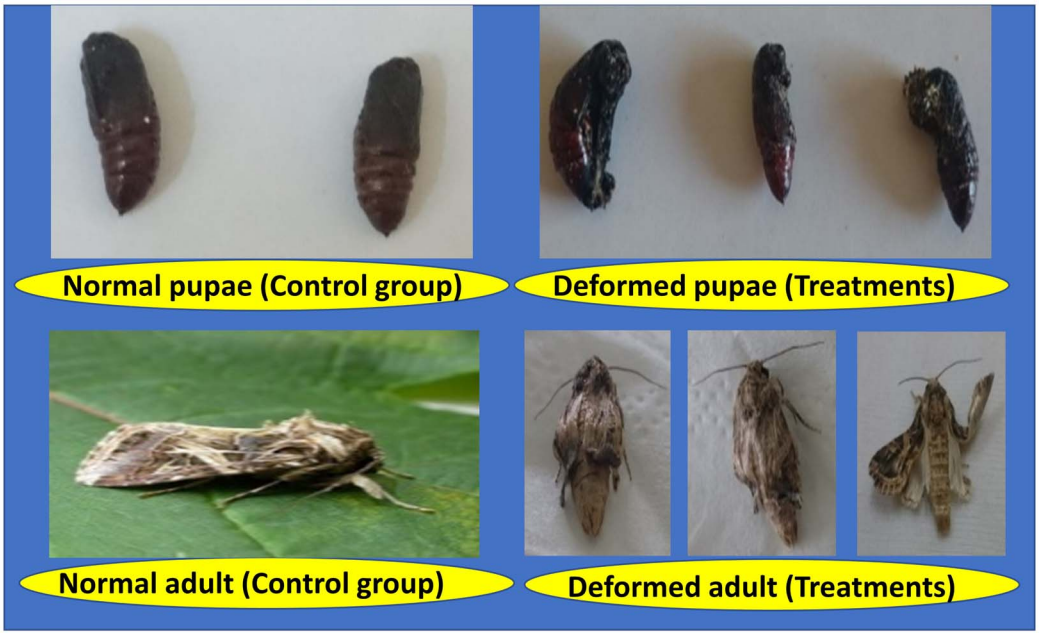

Fig. 6 Abnormalities in both pupae and adults compared with the untreated groups.

offspring generation after exposure of the parent 4th instar larvae with **11**, the ultimate operative insecticide recording a significant reduction resultant in 731.67 eggs/female, 25.41% fecundity, and 43.67% fertility, followed by **5** (827.33 eggs/female, 28.73% fecundity, and 54.17% fertility), **13** (1014.33 eggs/female, 35.23% fecundity, and 61.81% fertility), **3** (1326.33 eggs/female, 46.06% fecundity, and 74.27% fertility) and **1** (1907.67 eggs/female, 66.25% fecundity, and 87.60% fertility), compared to untreated group (2879.67 eggs/female, 100% fecundity, and 98.37% fertility) (Fig. 5). The distortion in fecundity may well be owed to disfunction of development of an insect egg, which dependent on the constituents that are acquired by the ovary, which enfolds lipids, protein and carbohydrates, all of which are essential for embryonic assemblages. Also, the tabulated data in Table 6 and Fig. 5, 6 exposed that the examined new quinolinone insecticides, **11**, **5**, **13**, **3** and **1**, presented a notable reduction in adult longevity of both males and females. Compound **11** was the vastly energetic, promising powerful considerably decrease of adult male and female longevity to average 4.95 and 6.93 days, respectively, as compared to the untreated larvae (13.32 and 15.58 days), followed by **5** (6.96 and 10.17 days), **13** (9.07 and 10.58 days), **3** (9.79 and 11.61 days) and **1** (12.61 and 12.85 days).

2.2.3. Antioxidant activity. Also, increased generation of compounds containing reactive oxygen and nitrogen species (ROS and RNS) improves the ability of antioxidant and their biochemical aspects.[64,65] So that, synthesized compounds revealed varying levels of antioxidant activity compared to ascorbic acid as potent standard as shown in Table 7. Thus, compounds **12**, **11**, and **5** displayed high antioxidant potency, and this result stands up with values of electrochemical parameters E_{gap}, S, η and IP: small E_{gap}, high softness with low hardness and higher ionization energy values. Compounds **8** and **3** showed moderate antioxidant activity and the rest of the tested compounds **2** and **10** showed weak antioxidant activity that stood up with values of electrochemical parameters.

Compound **13** has the highest value in percentage of inhibition (94.38%) which may be attributed to pyrazolone moiety; furthermore, research has revealed that certain pyrazolone derivatives possess strong antioxidant properties.[66–68] Antioxidants work to prevent or slowdown cellular damage by intercepting or neutralizing free radical reactions.[69] They achieve this by reacting with free radicals at a quicker pace than the free radicals would with the substrate involving two mechanisms: sequential electron transfer proton transfer (SETPT) and hydrogen atom transfer (HAT). Whereas, the SETPT mechanism entails the antioxidant transferring an electron to the free radical (R), resulting in the formation of an antioxidant radical cation and an anion followed by a proton transfer from the radical cation to the anion (eqn. (1) and (2)).[70]

Table 7 Free radical scavenging activity of quinolinone derivatives (DPPH)

Tested Comps	Absorb (λ)	Inhibition (%)
Ascorbic acid	**0.053**	**90.27**
1	0.149	65.13
2	0.226	47.07
3	0.091	78.69
5	0.073	82.90
8	0.149	65.11
10	0.399	6.55
11	0.106	75.18
13	**0.024**	**94.38**

$$\text{(Antioxidant) H} + {}^{\bullet}\text{R} \rightarrow \text{(antioxidant) H}^{\bullet+} + \text{R}^{-} \quad (1)$$

$$\text{(Antioxidant) H}^{\bullet+} + \text{R}^{-} \rightarrow \text{(antioxidant) + RH} \quad (2)$$

2.3. Theoretical approaches and structure–activity relationship (SAR)

The design of synthesized molecular compounds can be predicted through computational chemistry methods, which serve as a compelling protocol for assessing their stability and calculating various structural parameters (Fig. 7 and 8). The Gaussian 09 program package was employed to evaluate cluster calculations using the B3LYP exchange functional in conjunction with DFT at the 6-311G(d,p) basis set level. This combination was used to perform DFT calculations on the synthesized compounds. Additionally, quantum chemical calculations, such as the energies of the highest occupied molecular orbital (HOMO) and lowest unoccupied molecular orbital (LUMO), revealed that the energy gap between these frontier orbitals ($E_{\text{HOMO}} - E_{\text{LUMO}}$) is an important stability index and influences the biological activities of the molecules. In contrast, compounds with smaller energy gaps are more polarized and are classified as soft molecules. Soft molecules exhibit greater reactivity than hard molecules due to their propensity to readily donate electrons to an acceptor.[39–41]

$$\Delta E = (E_{\text{HOMO}} - E_{\text{LUMO}}) \quad (3)$$

$$S = 1/2\eta \quad (4)$$

$$\eta = 1/2(E_{\text{HOMO}} - E_{\text{LUMO}}) \quad (5)$$

$$\text{IP} = -E_{\text{HOMO}} \quad (6)$$

Ionization potential (IP) is the energy required to grapping an electron from a neutral atom or molecule in their ground states. In the context of bioactive compounds, arranging them based on their ionization potential values can provide insights into their reactivity and potential biological effects. Generally, molecules with lower ionization potentials are more reactive and tend to participate in electron transfer processes more readily. Here's how you can arrange bioactive compounds based on their ionization potential values.

Additionally, the practical outcomes of the synthesized compounds are aligned with the obtained theoretical calculations by assessing the energy difference (E_{gap}), as an indicating factor of biological activity. The reduced energy gap values could be attributed to certain groups entering conjugation within these molecules. Consequently, the E_{gap} for the most highly bioactive synthesized molecules with significant antioxidant properties was established. For instance, the energy gap of compound **13** was smaller than other compounds also its IP is high (IP = 6.332 eV), indicating this compound enhanced its antioxidant potency (94.38%) than other synthesized molecules (6.55–82.90%) and is superior to the standard drug (ascorbic acid, 90.27%). This postulation agrees with the data of the calculated parameters, which may be due to the presence of pyrazole moiety.

The superior efficacy of compound **11** compared to other test compounds may be attributed to the presence of the pyrazole moiety and the three nitrogen atoms enhanced the antioxidant activity.[71] Whereas, compound **10** showed lower antioxidant activity than others due to the absence of pyrazole or pyrazalone moieties; this postulate verifies that the most essential lead moieties in the synthesized compounds are pyrazole or pyrazalone moieties.

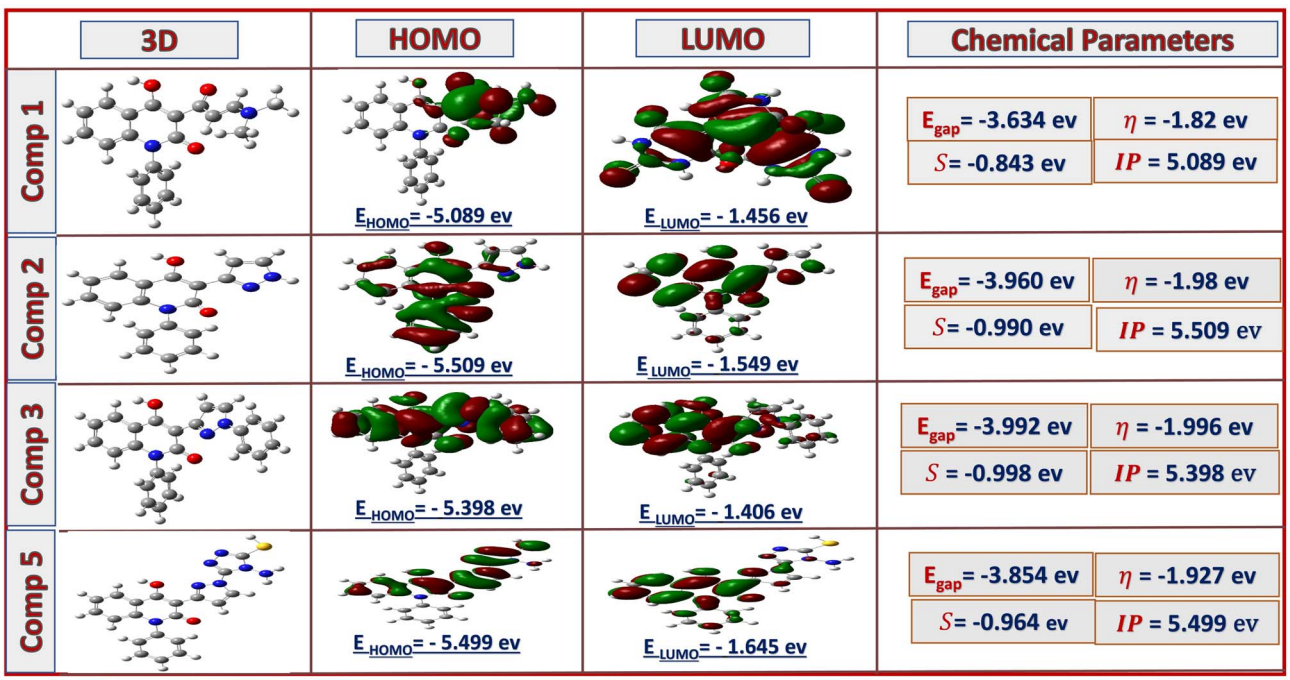

Fig. 7 Optimized structures of **1–3**, **5** and their electrochemical parameters.

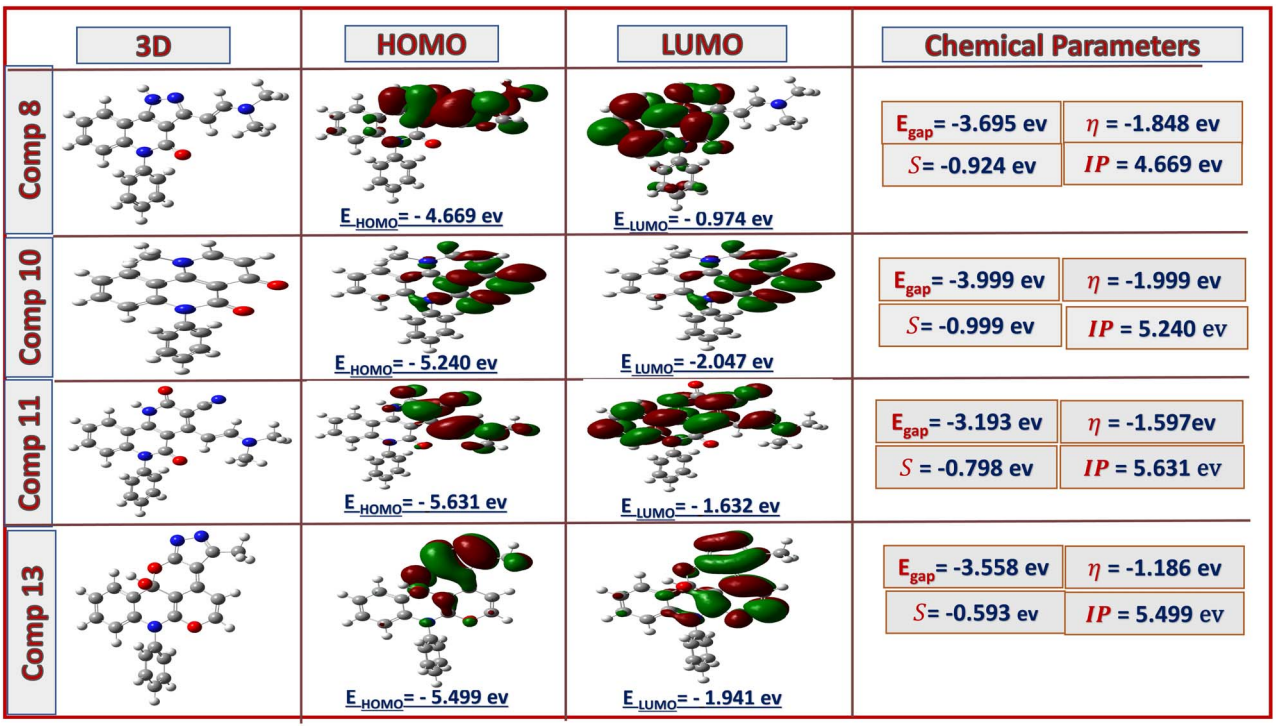

Fig. 8 Optimized structures **8**, **10**, **11**, **13** and their electrochemical parameters.

3. Experimental

3.1. Chemistry

All devices, equipment, materials, and methods are shown and discussed in detail in the DAS.

3.1.1. General procedure for synthesis of compounds 2, 3, 5, 8, 11 and 13. Equimolar amount of enaminone **1** (0.334 g, 1 mmol) and appropriate reagent in ethanol (15 ml) with catalytic amount of glacial acetic acid (2 ml) was refluxed for 1 h. The reaction mixture was left to cool at room temperature then poured onto crushed ice to give solid deposits. The product was filtered, washed by water to get rid of extra acid then recrystallized from EtOH and DMF.

3.1.2. 4-Hydroxy-1-phenyl-3-(1*H*-pyrazol-3-yl)quinolin-2(1*H*)-one (2). Yield, 87%; white sheets; mp > 300 °C; [EtOH : DMF (3 : 1)]; $R_f = 0.53$ [pet ether : ethyl acetate (2 : 1)]; FTIR (KBr) ν_{max}, cm^{-1}: 3188 (br, OH and NH), 3038 ($CH_{aromatic}$), 1629 (C=O, lactamic); ^{1}H NMR (500 MHz, DMSO-d_6) δ 6.50 (d, $J = 8.0$ Hz, 1H), 7.20 (d, $J = 2.5$ Hz, 1H), 7.27 (t, $J = 7.2$ Hz, 1H), 7.34 (d, $J = 7.5$ Hz, 2H), 7.44 (t, $J = 7.2$ Hz, 1H), 7.55 (t, $J = 7.2$ Hz, 1H), 7.62 (t, $J = 7.5$ Hz, 2H), 7.94 (d, $J = 1.5$ Hz, 1H), 8.10 (d, $J = 7.5$ Hz, 1H), 13.45 and 14.12 (2 s, 2H, OH, NH, exchangeable D_2O); ^{13}C NMR (125 MHz, DMSO-d_6) $\delta = 160.6$ (1C), 159.9 (1C), 148.0 (1C), 139.5 (1C), 138.0 (1C), 131.1 (1C), 129.9 (2C), 129.4 (3C), 129.2 (1C), 128.5 (1C), 123.5 (1C), 121.9 (1C), 115.2 (1C), 105.1 (1C), 100.5 (1C); (EIMS) *m*/*z* (%): 303.07 (M^+, 17.94), 283.91 (94.00), 264.33 (89.06), 261.99 (96.39), 209.90 (base peak, 100), 204.88 (84.22), 119.78 (92.46), 65.26 (97.37); anal. calcd. For $C_{18}H_{13}N_3O_2$ (303.32): C, 71.28; H, 4.32; N, 13.85; found: C, 71.26; H, 4.34; N, 13.82%.

3.1.3. 4-Hydroxy-1-phenyl-3-(1-phenyl-1*H*-pyrazol-3-yl)quinolin-2(1*H*)-one (3). Yield, 82%; yellow powder; mp = 259–260 °C; [EtOH : DMF (3 : 1)]; $R_f = 0.63$ [pet ether : ethyl acetate, (4 : 2)]; FTIR (KBr) ν_{max}, cm^{-1}: 3140 (br, OH), 3043 (CH olefinic), 1642 (C=O, lactamic); ^{1}H NMR (500 MHz, DMSO-d_6) δ 6.49 (d, $J = 2.4$ Hz, 1H), 7.04 (d, $J = 6.4$ Hz, 1H), 7.21–7.27 (m, 2H), 7.37 (t, $J = 7.6$ Hz, 2H), 7.42–7.47 (m, 5H), 7.49 (t, $J = 7.6$ Hz, 1H), 7.56 (t, $J = 7.3$ Hz, 2H), 7.75 (d, $J = 1.5$ Hz, 1H), 8.00 (d, $J = 7$Hz, 1H), 11.04 (s, 1H, OH, exchangeable D_2O); ^{13}C NMR (DMSO-d_6, 125 MHz): δ 161.0 (1C), 159.7 (1C), 140.4 (1C), 139.8 (1C), 137.6 (1C), 134.2 (1C), 131.5 (2C), 130.0 (2C), 129.9 (1C), 128.7 (1C), 128.5 (3C), 126.9 (1C), 123.8 (1C), 123.0 (1C), 121.8 (2C), 115.4 (1C), 115.2 (1C), 110.2 (1C), 102.4 (1C); (EIMS) *m*/*z* (%): 379.22 (M^+, 57.07), 369.015 (69.47), 302.38 (67.07), 286.80 (base peak, 100), 275.04 (69.87), 271.97 (63.97), 77.17 (64.74), 68.88 (75.45); anal. calcd. for $C_{24}H_{17}N_3O_2$ (379.42): C, 75.98; H, 4.52; N, 11.08; found: C, 75.97; H, 4.54; N, 11.11%.

3.1.4 3-(1-(4-Amino-5-mercapto-4*H*-1,2,4-triazol-3-yl)-1*H*-pyrazol-3-yl)-4-hydroxy-1-phenylquinolin-2(1*H*)-one (5). Yield, 87%; golden yellow flakes; mp = 278–280 °C; [EtOH : DMF (3 : 1)]; $R_f = 0.42$ [pet ether : ethyl acetate, (2 : 1)]; FTIR (KBr) ν_{max}, cm^{-1}: 3409 (br, OH), 3308 (NH_2), 1628 (C=O, lactamic); ^{1}H NMR (500 MHz, DMSO-d_6) δ 5.86 (s, 2H, NH_2, exchangeable D_2O), 6.53 (d, $J = 8.0$ Hz, 1H), 7.31 (t, $J = 7.7$ Hz, 1H), 7.37 (d, $J = 7$ Hz, 2H), 7.48–7.51 (m, 2H), 7.56 (t, $J = 7.2$ Hz, 1H), 7.63 (t, $J = 7.7$ Hz, 2H), 8.12 (d, $J = 8.0$ Hz, 1H), 8.60 (d, $J = 3$ Hz, 1H), 13.07 (s, 1H, OH, exchangeable D_2O), 14.15 (s, 1H, SH, exchangeable D_2O); ^{13}C NMR (DMSO-d_6, 125 MHz): δ 167.3 (1C), 160.9 (1C), 160.5 (1C), 151.4 (1C), 144.0 (1C), 139.9 (1C), 137.7 (1C), 132.5 (1C), 132.0 (1C), 130.0 (2C), 129.3 (2C), 128.7 (1C), 123.8 (1C),

122.2 (1C), 115.4 (1C), 114.8 (1C), 108.7 (1C), 99.4 (1C); (EIMS) *m*/*z* (%): 417.03 (M^+, 22.26), 308.34 (44.35), 255.89 (93.43), 233.38 (45.29), 196.54 (46.42), 103.40 (46.03), 59.27 (57.92), 43.10 (base peak, 100); anal. calcd. For $C_{20}H_{15}N_7O_2S$ (417.10): C, 57.55; H, 3.62; N, 23.49; S, 7.68%; found: C, 57.58; H, 3.61; N, 23.47; S, 7.66%.

3.1.5. (*E*)-3-(2-(Dimethylamino)vinyl)-5-phenyl-2,5-dihydro-4*H*-pyrazolo[4,3-*c*]quinolin-4-one (8). Yield, 73%; orange powder; mp = 256–258 °C; [EtOH : DMF (3 : 1)]; R_f = 0.64 [pet ether : ethyl acetate (1 : 1)]; FTIR (KBr) ν_{max}, cm^{-1}: 3138 (NH), 2927 (C–$H_{aliphatic}$), 1634 (C=O, lactamic); ^{1}H NMR (DMSO-d_6, 500 MHz): δ 2.93 (s, 3H, CH_3), 3.26 (s, 3H, CH_3), 6.37 (d, J = 8 Hz, 1H), 6.90–6.94 (m, 1H), 7.18 (t, J = 7.2 Hz, 1H), 7.29 (d, J = 7.5 Hz, 2H), 7.44 (t, J = 7.2 Hz, 1H), 7.51 (d, J = 7 Hz, 1H), 7.58 (t, J = 7.2 Hz, 2H), 8.09 (d, J = 7 Hz, 1H), 8.21 (d, J = 12 Hz, 1H), 8.42 (s, 1H, NH, exchangeable D_2O); ^{13}C NMR (DMSO-d_6, 125 MHz): δ 185.3 (1C), 178.1 (1C), 157.2 (1C), 138.2 (1C), 133.2 (1C), 129.9 (4C), 129.6 (4C), 128.4 (1C), 125.1 (1C), 121.5 (1C), 115.3 (1C), 92.0 (1C), 45.5 (1C), 37.6 (1C); (EIMS) *m*/*z* (%): 330.52 (M^+,15.38), 329.65 (35.98), 313.34 (57.95), 177.85 (57.52), 116.01 (39.42), 79.77 (47.99), 66.80 (31.14), 42.26 (base peak, 100); anal. Calcd. For $C_{20}H_{18}N_4O$ (330.39): C, 72.71; H, 5.49; N, 16.96%; found: C, 72.74; H, 5.47; N, 16.92%.

3.1.6 1-Methyl-6-phenylbenzo[*h*][1,6]naphthyridine-4,5(1*H*,6*H*)-dione (10). A mixture of enaminone **1** (0.334 g, 1 mmol), TETA (0.15 ml, 1 mmol) was stirred in CH_2Cl_2 at room temperature. Excess CH_2Cl_2 was removed by evaporation; gave the product then recrystallized from EtOH. Yield, 43%; off white powder; mp > 300 °C; [EtOH]; R_f = 0.84 [pet ether : ethyl acetate (4 : 3)]; FTIR (KBr) ν_{max}, cm^{-1}: 3055 (C–H), 1655 (C=O), 1601 (C=O, lactamic); ^{1}H NMR (400 MHz, DMSO-d_6) δ 2.70 (s, 3H, CH_3), 6.50 (d, J = 8 Hz, 1$H_{Olefinic}$), 7.33–7.37 (m, 4H), 7.58–7.65 (m, 5H_{Ar}), 8.18 (d, J = 8 Hz, 1$H_{Olefinic}$);^{13}C NMR (100 MHz): δ 206.8 (1C), 174.6 (1C), 142.9 (1C), 137.8 (1C), 135.6 (1C), 130.5 (3C), 129.7 (3C), 129.3 (1C), 125.7 (1C), 122.9 (1C), 116.2 (2C), 114.7 (1C), 106.3 (1C), 31.3 (1C); (EIMS) *m*/*z* (%): 302.31 (M^+, 30.89), 298.96 (62.42), 269.17 (base peak, 100), 222.34 (73.81), 177.17 (57.72), 148.62 (90.69), 120.60 (63.70), 68.45 (57.87); anal. calcd. For $C_{19}H_{14}N_2O_2$, added molecular weight 302.33: C, 75.48; H, 4.67; N, 9.27; O, 10.58; found: C, 75.46; H, 4.65; N, 9.39%.

3.1.7 (*E*)-4-(2-(Dimethylamino)vinyl)-2,5-dioxo-6-phenyl-1,2,5,6-tetrahydrobenzo [*h*][1,6]naphthyridine-3-carbonitrile (11). Yield, 56%; pale orange mp = 218–220 °C; [EtOH]; R_f = 0.55 [pet ether : ethyl acetate (1 : 1)]; FTIR (KBr) ν_{max}, cm^{-1}: 3465 (NH), 3058 (C–$H_{olefinic}$), 2930 (C–$H_{aliphatic}$), 2225 (CN), 1636 (C=O, lactamic), 1606 (C=O, lactamic); ^{1}H NMR (DMSO-d_6, 500 MHz): δ 2.93 (s, 3H, CH_3), 3.27 (s, 3H, CH_3), 6.36 (d, J = 5 Hz, 1H), 6.91 (d, J = 9 Hz, 1H), 7.18 (t, J = 7.2 Hz, 1H), 7.29 (d, J = 6.5 Hz, 2H), 7.44 (t, J = 7.5 Hz, 1H), 7.51 (t, J = 7 Hz, 1H), 7.58 (t, J = 7.7 Hz, 2H), 8.09 (d, J = 7.5 Hz, 1H), 8.21 (d, J = 12 Hz, 1H), 16.77 (s, 1H, NH, exchangeable D_2O); ^{13}C NMR (DMSO-d_6, 125 MHz): δ 157.2 (2C), 133.2 (1C), 130.0 (6C), 129.6 (5C), 128.4 (2C), 125.2 (1C), 121.5 (1C), 115.3 (2C), 92.1 (1C), 45.5 (1C), 37.7 (1C); (EIMS) *m*/*z* (%): 382.68 (M^+, 16.86), 335.04 (61.43), 327.96 (57.82), 321.48 (51.07), 282.56 (49.84), 280.8 (base peak, 100), 275.78 (82.74), 161.68 (42.43), 109.47 (45.97); anal. calcd. For $C_{23}H_{18}N_4O_2$ (382.42): C, 72.24; H, 4.74; N, 14.65; found: C, 72.21; H, 4.76; N, 14.67%.

3.1.8. 3-Methyl-7-phenyl-6,12-dioxa-1,2,7-triazaindeno [4,5,6-*de*]anthracen-11*b*(7*H*)-ol (13). Yield, 68%; pall yellow powder; mp = 234–236 °C; [EtOH : DMF (5 : 1)]; R_f = 0.74 [pet ether : ethyl acetate (1 : 1)]; FTIR (reflectance) ν_{max}, cm^{-1}: 3070 (C–H, olefinic), 2983 (C–H, aliphatic), 1633 (C=N); ^{1}H NMR (400 MHz, DMSO-d_6) δ 2.30 (s, 3H, CH_3), 3.37 (OH, contaminated with H_2O of DMSO), 6.43 (d, J = 8.4 Hz, 1H), 7.27 (t, J = 14.4 Hz, 1H), 7.34 (d, J = 18.8 Hz, 2H), 7.56–7.63 (m, 4H), 7.97 (d, J = 15.2 Hz, 1H), 8.16 (d, J = 7.2, 1H), 8.33 (d, J = 13.6 Hz, 1H); (EIMS) *m*/*z* (%): 369.43 (M^+, 29.25), 271.51 (73.94), 223.52 (38.33), 151.18 (66.25), 149.54 (33.36), 140.94 (57.20), 116.75 (40.37), 112.80 (base peak, 100); anal. calcd. For $C_{22}H_{15}N_3O_3$, added molecular weight 369.38: C, 71.54; H, 4.09; N, 11.38; Found: C, 71.59; H, 4.07; N, 11.36%.

3.2. Insecticidal activities

S. littoralis laboratory strain was obtained from the cotton leafworm research department, plant protection institute, Dokki, Giza. In addition, the wingless *A. gossypii* species were selected at random cotton fields to fresh Castor leaves. Whereby, *Neonate nymphs* were used in the experiments.[72] Whereby, acetamiprid 20% SP was obtained from Shandong Leeder Cropscience, LTD, China.

Bioassay experiments for the insecticidal bioactivity of inventive quinolinone scaffolds were conducted at different concentrations against the freshly molted 2nd and 4th instar larvae of *S. littoralis*[73] as well as neonate nymphs of *A. gossypii*.[74] Whereas, Larval mortality was calculated *via* using Abbotts formula.[75] In addition, statistical Finney method[76] was utilized to get the LC_{25} and LC_{50} values of inspected quinolinones. Whereby, the toxicity index was calculated by Sun equation.[77]

The impacts of the examined quinolinones on the insect's enzymatic profile (AChE, ATPase, total protein, CaE, GST) were assigned according to published protocols.[39,78] Leaves of the caster bean were immersed in LC_{25} of each tested pesticide and utilized for the nourishment of 4th instar larvae. Three hundred larvae were used for each tested compound.[78] The efficacy of the estimated synthetic pyrazoloquinolinone compounds **11**, **5**, **13**, **3**, and **1**, utilizing the leaf-dip technique at their LC_{25} values, on larval and pupal duration, pupal weight, percentage of normal, deformed pupae, adult emergence, fecundity (number of eggs per female), fertility (percentage of egg hatchability), and adult longevity (from emergence until death for both male and female) for surviving fourth instar larvae of the *S. littoralis* laboratory strain were assessed. As the fecundity percentage was determined using the method established by Crystal and Lachance[79] according to the following equation:

$$\%\ \text{fecundity} = \frac{\text{no. eggs(treated female)}}{\text{no. eggs(untreated female)}} \times 100 \qquad (7)$$

3.3. Statistical analysis

All biological aspects were analyzed *via* SPSS 13.0 package, whereby Duncan's test was used to determine the probability level comparing the differences among parameter means (P < 0.05) by the Costat program.[80]

4. Conclusions

Concisely, we have orchestrated several Fused/binary pyrazole quinolinone hybrids *via* the tandem reactions of dimethylamino-4-hydroxy-1-phenylquinolinone **1** as dynamic building block with various nucleophiles hybrids such as hydrazine hydrate, phenylhydrazine, hydrazinyltriazole, hydrazinylbenzo[*d*]imidazole **6**, chromenecarbohydrazide **7** and active methylene compounds as malononitrile and pyrazolone **12**. Additionally, their insecticidal efficacy against *S. littoralis* and *A. gossypii* were evaluated. Further studies on the insecticidal toxicity, biochemical efficacy and the latent effect of pyrazoloquinolinones against two destructive and most harmful pests. Whereby, the insecticidal activities of the most effective quinolinone hybrids were decreased in the order of **11**, **5**, **13**, **3** and **1**, respectively. After that, the antioxidant properties of pyrazolopyridine scaffolds were screened revealing intriguing potent activity of fused pentacyclic **13** (94.37%) compared by ascorbic acid as common standard (90.27%). Whereas, the antioxidant efficacy order of latent scaffolds was lessened as seen in the order of **5**, **3**, **11**, **1**, and **8**, respectively. The quantum simulations for the synthesized scaffolds involving chemical potential, electrophilicity, hardness and softness properties are determined *via* using DFT as a powerful tool for deciphering insecticidal and antioxidant efficacy.

Data availability

The authors confirm that the data supporting the findings of this study are available within the article and its ESI materials.†

Author contributions

N.·N. E.: organic synthesis methodology, software, formal analysis; W.·S.·H: supervision, conceptualization, investigation, project administration, writing – original draft & editing, validation; M. A.: biological methodology, biological statistics, writing – original draft; E. A. G.: organic synthesis methodology, software, formal analysis, investigation, writing – original draft & editing; all authors reviewed the manuscript.

Conflicts of interest

There are no conflicts to declare.

Acknowledgements

The authors are thankful to Mansoura University, Egypt, for their support under project IDMU-SCI-23-64.

References

1 (*a*) S. K. Ramadan, D. R. A. Haleem, H. S. Abd-Rabboh, N. M. Gad, W. S. Abou-Elmagd and D. S. Haneen, *RSC Adv.*, 2022, **12**, 13628–13638; (*b*) W. S. Hamama, M. E. Ibrahim, A. A. Gooda and H. H. Zoorob, *RSC Adv.*, 2018, **8**, 8484–8515.
2 E. A. Ghareeb, N. F. Mahmoud, E. A. El-Bordany and E. A. El-Helw, *Bioorg. Chem.*, 2021, **112**, 104945.
3 E. A. El-Helw, E. M. Hosni, M. Kamal, A. I. Hashem and S. K. Ramadan, *Bioorg. Chem.*, 2024, **150**, 107591.
4 S. Lawrance, S. Varghese, E. M. Varghese, A. K. Asok and M. S. Jisha, *Biocatal. Agric. Biotechnol.*, 2019, **18**, 101096.
5 P. Cui, K. Liu, Z. Yang, P. Sun, Y. Meng, Q. Yang, X. Wu, Y. Lv, Y. Yang and J. Wu, *ACS Omega*, 2024, **9**, 36671–36681.
6 Y. L iu, S. Du, X. Xu, L. Qiu, S. Hong, B. Fu and Z. Qin, *J. Agric. Food Chem.*, 2024, **72**, 3342–3353.
7 Q. Cai, H. Song, Y. Zhang, Z. Zhu, J. Zhang and J. Chen, *J. Agric. Food Chem.*, 2024, **72**, 12373–12386.
8 J. Yang, S. W. Chen, B. Zhang, Q. Tu, J. Wang and M. S. Yuan, *Talanta*, 2022, **240**, 123200.
9 M. Abass and B. B. Mostafa, *Bioorg. Med. Chem.*, 2005, **13**, 6133–6144.
10 K. Hemalatha, G. Madhumitha, A. Kajbafvala, N. Anupama, R. Sompalle and S. M. Roopan, *J. Nanomater.*, 2013, 341015.
11 B. Guo, L. Chen, S. Luo, C. Wang, Y. Feng, X. Li, C. Cao, L. Zhang, Q. Yang, X. Zhang and X. Yang, *J. Agric. Food Chem.*, 2024, **72**, 10271–10281.
12 C. Vidau, J. Brunet, A. Badiou and L. P. Belzunces, *Toxicol. in Vitro*, 2009, **23**, 589–597.
13 Z. Yating, G. Zhanyu, X. Jing, L. Bingzhi, Q. Peiwen and J. Mingshan, *Chin. J. Pestic. Sci.*, 2024, **26**, 716–723.
14 D. Liu, J. Ye, Y. Gao, H. Pei, C. Luo, H. Tian, H. Tian, J. He, J. Zhang and L. Zhang, *J. Agric. Food Chem.*, 2024, **72**, 15276–15283.
15 C. Chang, S. Dai, C. Chen, L. Huang, Y. Chen and J. Hsu, *Pestic. Biochem. Physiol.*, 2024, **203**, 106001.
16 Y. Li, M. Li, N. Shakoor, Q. Wang, G. Zhu, Y. Jiang, Q. Wang, I. Azeem, Y. Sun, W. Zhao, L. Gao, P. Zheng and Y. Rui, *J. Agric. Food Chem.*, 2024, **72**, 22985–23007.
17 V. S. Lucena-Leandro, E. F. A. Abreu, L. A. Vidal, C. R. Torres, C. I. V. F. Junqueira, J. Dantas and E. V. S. Albuquerque, *Int. J. Mol. Sci.*, 2022, **23**, 15836.
18 W. S. Hamama, G. G. El-Bana, M. E. H. Mostafa and H. H. Zoorob, *J. Heterocycl. Chem.*, 2019, **56**, 239–250.
19 H. M. Lisboa, A. Nascimento, A. Arruda, A. Sarinho, J. Lima, L. Batista, M. F. Dantas and R. Andrade, *Foods*, 2024, **13**, 1846.
20 R. Arora and S. Sandhu, *Breeding Insect Resistant Crops for Sustainable Agriculture*, Publisher: Springer, 1st edn, 2017, pp. 467, Singapore ISBN: 978981106, DOI: DOI: **10.1007/978-981-10-6056-4**.
21 E. S. H. Shaurub, A. E. Abdel Aal and S. A. Emara, *Reprod. Dev.*, 2020, **64**, 178–187.
22 U. Naeem-Ullah, M. Ramzan, S. H. M. Bokhari, A. Saleem, M. A. Qayyum, N. Iqbal and S. Saeed, Insect Pests of Cotton Crop and Management Under Climate Change Scenarios, *Environment, Climate, Plant and Vegetation Growth*, 2020, pp. 367, DOI: DOI: **10.1007/978-3-030-49732-3_15**.
23 R. Kaur, D. Choudhary, S. Bali, S. S. Bandral, V. Singh, M. A. Ahmad, N. Rani, T. G. Singh and B. Chandrasekaran, *Sci. Total Environ.*, 2024, **915**, 170113.

24 W. J. Pitt, L. R. Kairy, V. Mora, E. Peirce, A. S. Jensen, B. Bradford, R. Groves, T. Christenesen, I. Macrae and P. Nachappa, *J. Appl. Ecol.*, 2024, **61**, 1573–1586.
25 V. Rakesh, V. Rajesh, A. Jeevalatha and A. Ghosh, Exploring the Relationship of Potato Viruses with Aphid and Whitefly Vectors, in *Approaches for Potato Crop Improvement and Stress Management*, Springer Nature Singapore. Singapore, 2024, vol. 249.
26 J. Shang, H. Wang, W. Dong, X. Guo, J. Zhu, P. Liang and X. Shi, *Pestic. Biochem. Physiol.*, 2024, **205**, 106138.
27 M. Farhan, J. Pan, H. Hussain, J. Zhao, H. Yang, I. Ahmad and S. Zhang, *Plants*, 2024, **13**, 2332.
28 Z. Hamouche, C. Zippari, A. Boucherf, G. Cavallo, K. Djelouah, G. Tamburini and D. Cornara, *CABI Agric. Biosci.*, 2024, **5**, 61.
29 C. A. Dedryver, A. Le Ralec and F. Fabre, *C. R. Biol.*, 2010, **333**, 539–553.
30 Y. Li, R. Li, H. Shao, Z. Liu, X. Gao, Z. Tian, Y. Zhang and J. Liu, *J. Agric. Food Chem.*, 2024, **72**, 25549–25559.
31 S. Manna, S. Roy, A. Dolai, A. R. Ravula, V. Perumal and A. Das, *Frontal Nanotechnol. Res.*, 2023, **4**, 1082128.
32 H. Zhou, Y. Jian, Q. Shao, F. Guo, M. Zhang, F. Wan, L. Yang, Y. Liu, L. Yang, Y. Li, P. Yang, Z. Li, S. Li and W. Ding, *J. Agric. Food Chem.*, 2023, **71**, 18359–18374.
33 X. P. Lu, L. Xu and J. J. Wang, *Pestic. Biochem. Physiol.*, 2024, **202**, 105964.
34 Q. Wei, X. Zhu, D. Zhang, H. Liu and B. Sun, *Trends Food Sci. Technol.*, 2024, 104636.
35 J. R. Lane, P. M. Sexton and A. Christopoulos, *Trends Pharmacol. Sci.*, 2013, **34**, 59–66.
36 A. K. Singh, A. Kumar, H. Singh, P. Sonawane, H. Paliwal, S. Thareja, P. Pathak, M. Grishina, M. Jaremko, A. H. Emwas, J. P. Yadav, A. Verma, H. Khalilullah and P. Kumar, *Pharmaceuticals*, 2022, **15**, 1071.
37 (*a*) G. L. Spada, D. V. Miniero, M. Rullo, M. Cipolloni, P. Delre, C. Colliva, F. Leonetti, G. M. Liuzzi, G. F. Mangiatordi, N. Giacche and L. Pisani, *Eur. J. Med. Chem.*, 2024, **274**, 116511; (*b*) A. Demirçal and T. Topal, *J. Mol. Struct.*, 2023, **1288**, 135782.
38 L. Wang, Y. Zhang, Y. Chen, P. Liu, Z. Ma, Y. Liu, L. Chen, L. Zheng and Q. Cao, *Talanta*, 2024, **280**, 126720.
39 E. A. Ghaith, H. A. Ali, M. A. Ismail, A. S. Fouda and M. Abd El Salam, *BMC Chem.*, 2023, **17**, 144.
40 E. A. Ghaith, H. H. Zoorob and W. S. Hamama, *Chem. Biodiversity*, 2024, **21**, e202400243.
41 E. A. Ghaith, H. H. Zoorob, M. E. Ibrahim, M. Sawamura and W. S. Hamama, *ChemistrySelect*, 2020, **5**, 14917–14923.
42 W. S. Hamama, E. A. Ghaith, M. E. Ibrahim, M. Sawamura and H. H. Zoorob, *ChemistrySelect*, 2021, **6**, 1430–1439.
43 I. J. Amaye, R. D. Haywood, E. M. Mandzo, J. J. Wirick and P. L. Jackson-Ayotunde, *Tetrahedron*, 2021, **83**, 131984.
44 S. Zilberg and B. Dick, *Phys. Chem. Chem. Phys.*, 2017, **19**, 25086–25094.
45 S. Zilberg and B. Dick, *ChemistrySelect*, 2016, **1**, 195–200.
46 V. C. Rufino and J. R. Pliego, *J. Braz. Chem. Soc.*, 2023, **34**, 1499–1508.
47 Z. Song, C. Zhu, k. Gong, R. Wang, J. Zhang, S. Zhao, Z. Li, X. Zhang and J. Xie, *J. Am. Chem. Soc.*, 2024, **146**, 10963–10972.
48 V. C. Rufino and J. Vohlídal, *J. Phys. Org. Chem.*, 2023, **36**, e4467.
49 (*a*) G. G. El-Bana, W. S. Hamama, H. H. Zoorob and M. E. Ibrahim, *Chem. Biodiversity*, 2023, e202300156; (*b*) R. Kumar, N. Kumari, H. Kaur, C. Bal and A. Sharon, *J. Heterocycl. Chem.*, 2023, **60**, 1641–1646.
50 B. Vermeeren, S. Van Praet, W. Arts, T. Narmon, Y. Zhang, C. Zhou, H. P. Steenackers and B. F. Sels, *Chem. Soc. Rev.*, 2024, **53**, 11804–11849.
51 I. Spanopoulos, W. Ke, C. C. Stoumpos, E. C. Schueller, O. Y. Kontsevoi, R. Seshadri and M. G. Kanatzidis, *J. Am. Chem. Soc.*, 2018, **140**, 5728–5742.
52 N. A. Ibrahim, S. A. El-Kaed, S. A Rizk and A. K. Ali, *Polycyclic Aromat. Compd.*, 2022, **42**, 5567–5584.
53 A. Bagherinejad and A. Alizadeh, *Org. Biomol. Chem.*, 2022, **20**, 7188–7215.
54 C. Praveenkumar, S. Pradeep and R. Pungavi, *Insect Physiology and Biochemistry: Mechanisms and Signalling Pathways*, 2024, eBook-ISBN: 9781003532569.
55 K. W. Beyenbach and P. M. Piermarini, *Osmotic and Ionic Regulation in Insects*, 2008, eBook-ISBN: 9780429126154.
56 A. Ponsankar, P. Vasantha-Srinivasan, A. Thanigaivel, E. S. Edwin, S. Selin-Rani, M. Chellappandian, S. Senthil-Nathan, K. Kalaivani, A. Mahendiran, W. B. Hunter, R. T. Alessandro, V. Duraipandiyan and N. A. Al-Dhabi, *Physiol. Mol. Plant Pathol.*, 2018, **101**, 16–28.
57 A. A. Aioub, A. S. Hashem, A. H. El-Sappah, A. El-Harairy, A. A. A. Abdel-Hady, L. A. Al-Shuraym, S. Sayed, Q. Huang and S. I. Z. Abdel-Wahab, *Toxics*, 2023, **11**, 542.
58 Y. Huang, Z. Xu, X. Lin, Q. Feng and S. Zheng, *J. Insect Physiol.*, 2011, **57**, 1033–1044.
59 F. Hilliou, T. Chertemps, M. Maïbèche and G. Le Goff, *Insects*, 2021, **12**, 544.
60 C. Cruse, T. W. Moural and F. Zhu, *Insects*, 2023, **14**, 194.
61 C. A. Farnsworth, M. G. Teese, G. Yuan, Y. Li, C. Scott, X. Zhang, Y. Wu, R. J. Russell and J. G. Oakeshott, *J. Pestic. Sci.*, 2010, **35**, 275–289.
62 M. A. M. Moustafa, E. A. Osman, E. M. S. Mokbel and E. A. Fouad, *Crop Prot.*, 2024, **177**, 106533.
63 P. H. Yao, S. H. Mobarak, M. F. Yang and C. X. Hu, *BMC Genomics*, 2025, **26**, 14.
64 R. Thiruvengadam, B. Venkidasamy, M. Easwaran, H. Y. Chi, M. Thiruvengadam and S. H. Kim, *Plant Cell Rep.*, 2024, **43**, 198.
65 P. S. A. Shankar, P. Parida, R. Bhardwaj, A. Yadav, P. Swapnil, C. S. Seth and M. Meena, *Plant Cell Rep.*, 2024, **43**, 185.
66 S. Mortada, K. Karrouchi, E. H. Hamza, A. Oulmidi, M. A. Bhat, H. Mamad and M. E. A. Faouzi, *Sci. Rep.*, 2024, **14**, 1312.
67 A. J. Hussein, *Curr. Org. Synth.*, 2024, **21**, 903–916.
68 Y. Li, Y. Luo, J. Wang, H. Shi, J. Liao, Y. Wang, Z. Cheng, L. Xiong, C. Chang and T. Wang, *Bioorg. Chem.*, 2023, **131**, 106283.

69 S. D. Meo and P. Venditti, *Oxid. Med. Cell. Longev.*, 2020, 9829176.
70 F. Azimi, M. Mahdavi, M. Khoshneviszadeh, F. Shafiee, M. Azimi, F. Hassanzadeh and F. H. Ashrafee, *Bioorg. Chem.*, 2024, **152**, 107722.
71 V. L. Silva, J. Elguero and A. M. Silva, *Eur. J. Med. Chem.*, 2018, **156**, 394–429.
72 J. Dampc, M. Kula-Maximenko, M. Molon and R. Durak, *Insects*, 2020, **11**, 436.
73 K. O. Rashid, K. S. Mohamed, M. A. E. Salam, E. Abdel-Latif, A. A. Fadda and M. R. Elmorsy, *Polycyclic Aromat. Compd.*, 2023, **43**, 356–369.
74 R. A. Reda, H. H. Nahla, A. S. Shereen and M. A. El-Salam, *Egypt. J. Plant Prot. Res. Inst.*, 2022, 382–394.
75 W. S. Abbott, *J. Econ. Entomol.*, 1925, **18**, 265–267.
76 D. J. Finney, *Probit Analysis: a Statistical Treatment of the Sigmoid Response Curve*, Cambridge University Press, 2nd edn, 1952.
77 Y. P. Sun, *J. Econ. Entomol.*, 1950, **43**, 45–53.
78 N. N. Soliman, M. Abd El Salam, A. A. Fadda and M. Abdel-Motaal, *J. Agric. Food Chem.*, 2020, **68**, 5790–5805.
79 M. M. Crystal and L. E. Lachance, *Biol. Bull.*, 1963, **125**, 270–279.
80 *Costat Program, Version 6.311*, Cohort Software Inc., Monterey, 2006, **https://www.cohort.com**.